

July 2021

Defining the Role of RBBP4 in Oocyte Maturation and Preimplantation Development Using Trim-Away

Holly L. Barletta
University of Massachusetts Amherst

Follow this and additional works at: https://scholarworks.umass.edu/masters_theses_2



Part of the [Animal Sciences Commons](#), [Biotechnology Commons](#), and the [Developmental Biology Commons](#)

Recommended Citation

Barletta, Holly L., "Defining the Role of RBBP4 in Oocyte Maturation and Preimplantation Development Using Trim-Away" (2021). *Masters Theses*. 1034.
<https://doi.org/10.7275/22946083.0> https://scholarworks.umass.edu/masters_theses_2/1034

This Open Access Thesis is brought to you for free and open access by the Dissertations and Theses at ScholarWorks@UMass Amherst. It has been accepted for inclusion in Masters Theses by an authorized administrator of ScholarWorks@UMass Amherst. For more information, please contact scholarworks@library.umass.edu.

**DEFINING THE ROLE OF RBBP4 IN OOCYTE MATURATION AND
PREIMPLANTATION DEVELOPMENT USING TRIM-AWAY**

A Thesis Presented

by

HOLLY L. BARLETTA

Submitted to the Graduate School of the
University of Massachusetts Amherst in partial fulfillment
of the requirements for the degree of

MASTER OF SCIENCE

May 2021

Animal Biotechnology and Biomedical Sciences

**DEFINING THE ROLE OF RBBP4 IN OOCYTE MATURATION AND
PREIMPLANTATION DEVELOPMENT USING TRIM-AWAY**

A Thesis Presented

by

HOLLY L. BARLETTA

Approved as to style and content by:

Wei Cui, Chair

Rafael Fissore, Member

Dominique Alfandari, Member

Cynthia Baldwin, ABBS Graduate Program
Director

AKNWOLEDGMENTS

I would like to thank Dr. Wei Cui for pushing me to always do my best and for helping me complete this thesis within a few short months and many very long days. Due to COVID-19, some plans got postponed and my thesis was changed halfway through this 5th year program, but with hard work, perseverance, and a great mentor it was possible to finish. I would like to thank the PhD student in my lab, Sue (Xiaosu) Miao, for not only guiding me through many experiments and classes, but for also being a great friend. I would like to thank my committee members Dr. Rafael Fissore and Dr. Dominique Alfandari for encouraging me to understand how research is conducted properly, and to continue to always ask questions. I would like to thank Neha Gupta and Ankit Pandey, PhD students from the Fissore Lab and Alfandari Lab respectively, for assisting me with some experiments and protocol optimization tips for my previous thesis topic and this current one. I would like to thank the UMass Amherst VASCI Department, especially Dr. Cynthia Baldwin, Dr. Katherine A. Beltaire, Dr. Susan Marston, and John Balise for providing me with so many fantastic opportunities throughout my time here as an undergraduate and graduate student. Lastly, I would like to thank all my friends and family who have been supporting me from day one, because there is no way I could get through this without them believing in me.

ABSTRACT

DEFINING THE ROLE OF RBBP4 IN OOCYTE MATURATION AND PREIMPLANTATION DEVELOPMENT USING TRIM-AWAY

MAY 2021

HOLLY L. BARLETTA, B.S., UNIVERSITY OF MASSACHUSETTS AMHERST
M.S., UNIVERSITY OF MASSACHUSETTS AMHERST

Directed by: Dr. Wei Cui

Retinoblastoma-binding protein 4 (RBBP4) is a subunit of chromatin remodeling factor 1 (CAF-1) and is essential for mammalian oocyte maturation, embryo survival, and embryo implantation. RBBP4 also localizes to the chromatin and is a ubiquitously expressed nuclear protein. Previous methods used to study this protein include short interfering RNAs (siRNAs) and CRISPR/Cas9. These techniques have limitations such as determining an indirect depletion of proteins, may trigger compensatory mechanisms, and may not be useful in non-dividing primary cells. A new, acute, and rapid endogenous protein depletion technique called Trim-Away, can overcome these limitations. Trim-Away is also widely applicable since it can be used with many off-the-shelf reagents. Trim-Away utilizes the TRIM21-antibody interaction within the cytosol and the ubiquitin-proteasome pathway (UPP) to target and degrade a protein of interest. Studying RBBP4 using Trim-Away can offer insight into possible new functions of RBBP4 and its maternal effect, and increase the knowledge on a new, acute, and endogenous protein depletion technique. Here we report that, RBBP4 is required for proper blastocyst development and RBBP4 is more abundant in MII oocytes than GVBD oocytes. We also report that the loss of RBBP4 hinders RNA synthesis and causes cell death in later stages

of embryo development. While our Trim-Away methodology can deplete RBBP4 as early as the 2-cell stage in embryos, our oocyte Trim-Away protocol needs to be optimized.

TABLE OF CONTENTS

ACKNOWLEDGMENTS iii

ABSTRACT..... iv

LIST OF TABLES viii

LIST OF FIGURES ix

CHAPTER

1. INTRODUCTION1

 A. Mammalian Oocyte Maturation.....1

 B. Fertilization, Maternal Effect Genes, and Preimplantation Embryo
 Development.....4

 C. Retinoblastoma-Binding Protein 4 (RBBP4).....6

 D. Trim-Away and TRIM219

 E. Aim of Study.....12

2. MATERIALS AND METHODS.....14

 A. Ethics statement and animal use14

 B. Oocyte and zygote collection.....14

 C. mRNA preparation.....15

 D. Microinjection.....17

 E. Immunofluorescence (IF).....19

 F. Live imaging20

 G. *In vitro* maturation (IVM) of oocytes20

 H. Western blot21

 I. 5-ethynyl uridine (EU) incorporation assay.....23

J. Terminal deoxynucleotidyl transferase dUTP nick end labeling (TUNEL)	23
3. RESULTS	24
A. Generation of mRNA	24
B. Trim-Away Methodology Confirmation	26
C. Trim-Away in Embryos	35
D. Total Nascent RNA	43
E. Total Cell Death	46
F. Trim-Away in Oocytes	47
4. DISCUSSION	55
BIBLIOGRAPHY	62

LIST OF TABLES

Table	Page
1. Plasmid Validation Buffers and Enzymes	16
2. Plasmid Linearization Buffers and Enzymes	17
3. mRNA and Antibody Microinjection Concentrations	18

LIST OF FIGURES

Figure	Page
1. Mouse Oocyte Maturation	3
2. Mouse Embryo Development	6
3. RBBP4 Signal from GV Oocytes to 2-cell Embryos.....	8
4. Trim-Away Schematic	12
5. Microinjection of Zygote	19
6. Wes Microplate Loading Schematic	22
7. pGEMHE-mEGFP-mTRIM21 and pGEMHE-mCherry-mTRIM21 RNA Purification.....	25
8. Co-injection of TRIM21 mRNA and Anti-RBBP4 in GV Oocytes	27
9. Separate Injections of TRIM21 mRNA and Anti-RBBP4 in GV Oocytes.....	27
10. Trim Away of H2B Using Unpurified Anti-H2B in MII Oocytes	29
11. Trim Away of H2B Using Purified Anti-H2B in MII Oocytes	30
12. Trim Away of H2B Using Purified Anti-H2B in Zygotes and 2-cell Embryos	31
13. Trim Away of H2B Using Purified Anti-H2B and Purified Anti-GFP	33
14. Trim-Away of MAP4 Using Purified Anti-MAP4 and Purified Anti-GFP.....	34
15. Trim-Away of RBBP4 At All Preimplantation Embryo Development Stages.....	37
16. Blastocyst Phenotype	43
17. EU Incorporation Assay Analysis.....	45
18. TUNEL of Morula Stage Embryos	47
19. Trim-Away of RBBP4 Using Anti-RBBP4 in Arrested GV Oocytes	48
20. Western Blot for RBBP4 Confirmation	50
21. Western Blot for Trim-Away During Oocyte Maturation	53

22. Electropherogram Quantification.....54

CHAPTER 1

INTRODUCTION

A. Mammalian Oocyte Maturation

William Harvey, M.D. (1578-1657), once stated “omne vivum ex ovo” or “all living things come from eggs,” which summarizes the importance of the oocyte in reproduction [1]. The maturation of a mammalian immature oocyte refers to the period of progression from the first to second meiotic arrest, ensures the capability of fertilization, and is the last phase of oogenesis [2, 3]. The oocyte needs to provide the developing embryo with the majority, if not all, of the molecular factors it will need until the embryonic genetic program is activated [1]. The maturation process involves tightly choreographed movements of chromosomes, activity of regulators and inhibitors, a high transcription rate, and many other factors through a specialized cell division process called meiosis [2, 4, 5]. Meiosis is unique to gametes (oocytes and sperm) and occurs during oocyte maturation, following steps for metaphase I (MI)/metaphase II (MII) spindle formation, the spindle assembly checkpoint (SAC), and chromosome segregation [4, 6]. Meiosis will progress continuously and will take about 12 hours in comparison to the 1 hour that mitosis does [4].

Normally, immature oocytes are arrested at the diplotene (fourth) stage of prophase I, also known as the germinal vesicle (GV) stage [7]. The GV is also known as the nucleus during the prophase stage [8]. In vivo, meiotic arrest is removed only after sexual maturity is reached and will differ between mammalian species [4]. During follicular growth within a female mouse, many ovarian follicles and cells within them respond to the luteinizing hormone (LH) surge for regulation of oocyte meiotic cell cycle

resumption[4]. This is restricted to oocytes which have reached full-size[7]. Once meiosis resumes, the disassembly of the GV/nuclear membrane called germinal vesicle breakdown (GVBD), occurs as the first morphological manifestation, and allows further maturation in the meiosis I process [4, 8]. Meiosis I will last for about 6-12 hours in mice going through stages such as prophase, prometaphase, MI, anaphase, telophase, and MII (Figure 1)[6]. During meiosis, oocytes undergo two consecutive asymmetric cytoplasm and symmetric nuclear divisions without an intervening S-phase (the DNA replication stage), to become germ cells which then contain half of the chromosomes previously present [9, 10]. At the MII stage, there is a division which consists of a large oocyte and a small polar body, a non-functional cell-like structure that degrades soon after it is extruded and will remain within the perivitelline space [7, 8]. This first polar body will be called polar body 1 (PBI) and after fertilization there will be a second polar body extruded called polar body 2 (PBII) [4]. The polar bodies extruded will include $\frac{3}{4}$ of supernumerary, or excess, chromosomes overall [11]. To ensure the success of offspring, appropriate chromosome segregation should take place during this process[12].

Pomerantz and Dekel make a point to state that any misstep within meiosis can cause aneuploidy and genetic malformations [4].

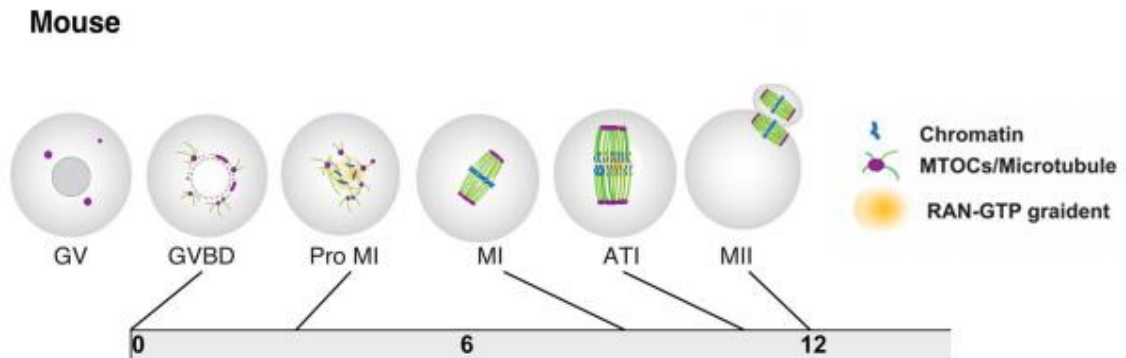


Fig 1. Mouse Oocyte Maturation (Adapted from[6])

Under in vitro maturation conditions, the maturation of the mouse oocyte from the GV stage to the MII stage is completed in around 12h, with GVBD occurring around 2h and MI around 6h.

Since germ cells are by far larger than somatic cells (mouse oocytes are around 70 μM while mouse epidermal cells are around 9 μM) they require additional steps of cellular reorganization such as spindle migration to the cortex via the microtubule organizing center (MTOC), the spindle assembly checkpoint (SAC), the mitogen-activated protein kinase (MAPK) pathway, and the ubiquitin proteasome pathway (UPP)[4, 6, 9, 13, 14]. The UPP plays an important role in protein degradation within living cells [4]. R oth and colleagues mentioned that the targeted protein of interest (POI) relies on recruitment of an E3 ligase for ubiquitination and degradation [15]. E3 ubiquitin ligases can be found within the UPP and will tag substrates with polyubiquitin chains for degradation. Ubiquitin chains are linked by a unique lysine residue serving as a cellular signal that is tagged onto the substrate to be recognized by the proteasome for degradation. This E3 ubiquitin ligase also plays an important role in the turnover of meiotic and mitotic proteins, and the regulation of the anaphase-promoting complex/cyclosome (APC/C) after GVBD for processes such as correct chromosome segregation during prometaphase I, and polar body extrusion [4].

When the oocytes reach MII, they will arrest again until fertilization under the influence of a cytostatic factor [4, 9]. Fertilization will trigger subsequent completion of the meiosis II division. The extrusion of the second polar body follows a calcium response from the sperm-egg fusion and opens the opportunity for recombination of maternal and paternal homologues to create new genetic combinations in the offspring [11].

B. Fertilization, Maternal Effect Genes, and Preimplantation Embryo Development

Preimplantation development of a mammalian embryo is considered the point from fertilization to the developmental stage of a blastocyst, in utero, and includes many morphological changes and lineage differentiations. Understanding the development and self-organization of the mouse embryo is important for further cell-reprogramming approaches[16].

Early preimplantation development embryos contain mRNA transcripts that are expressed from 2 different origins, maternal and zygotic. Maternal transcripts, also known as maternal genes, are deposited in the oocyte from the mother's genome, while the zygotic transcripts originate from the embryo's genome after fertilization. Maternal transcripts rely on post-translational regulatory mechanisms for their expression while zygotic transcripts can utilize both transcriptional and post-transcriptional regulatory mechanisms. The spatial and temporal expressions of each transcript are different for each origin. In mice, at least 30% of these protein-coding genes are expressed in the oocyte to embryo transition and can be divided into 3 groups; genes that are expressed exclusively from either the maternal or zygotic origin, genes that must be expressed by

both origins because of low mRNA stability or a change in spatial expression during transition from oocyte to zygote, and genes that can accommodate either maternal or zygotic expression [17].

Maternal-effect genes (MEGs) are involved in many processes throughout early embryo life such as gap-junction communication, DNA methylation status, and zygotic gene activation (ZGA). It has been shown with strong evidence that mammalian embryonic development depends on oocyte-derived factors which play essential roles as early as the zygote stage [18]. After fertilization, both parental genomes recombine and form a totipotent zygote through epigenetic remodeling. Before recombination, ZGA, and subsequent development, the many maternal factors need to unravel the parental genome from the protamines, instead of histones, that arrived in densely packed chromatin. Once the chromatin remodeling takes place, the development process can proceed [19]

Preimplantation development in mice stage takes several days, morphological changes, and lineage differentiations [16, 20]. Some of these changes include ZGA completed by the post translational modifications of the maternally inherited proteins at the 2-cell stage, and include compaction, polarization, and cavitation at the 8-cell stage [16, 21]. With further division, 2 distinct cell lineages then start to form: the trophectoderm (TE) and the inner cell mass (ICM), each with their own contributions to the embryo [16]. Transcription factors promote the different lineages so that the TE contributes to the placenta while the ICM contributes to all fetal cells and the embryonic yolk sac [16, 20]. The ICM then goes on to have a second lineage decision one day later [16]. There is differentiation for either becoming an extraembryonic monolayer that meets the blastocoel (primitive endoderm- PrE) or becoming the epiblast (EPI), which

gives rise to the embryo proper [20]. The developmental timeline for mouse preimplantation embryos can be seen in Figure 2.

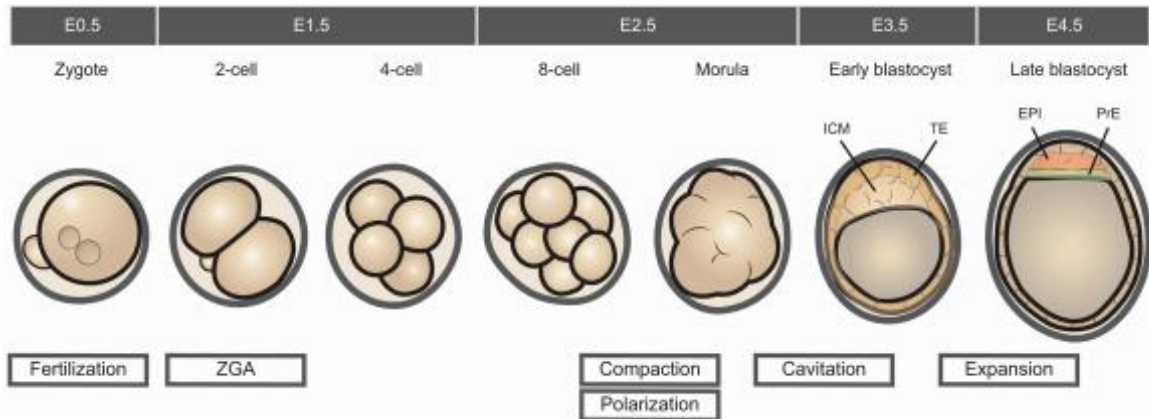


Fig 2. Mouse Embryo Development [20]

At embryonic day 0.5 (E0.5), fertilization, both the maternal and paternal nuclei are present and a total of 2 polar bodies have been extruded. At E1.5 the polar bodies start to degrade and the cell divides into the 2-cell and 4-cell stages while ZGA occurs. At E2.5 the embryo goes through compaction and polarization processes as it develops from the 8-cell stage to the morula stage. At E3.5, the blastocoel is present, and the embryo goes through cavitation creating the TE and ICM. At E4.5 the ICM is differentiated into the EPI and PrE when expansion occurs.

C. Retinoblastoma-Binding Protein 4 (RBBP4)

In addition, retinoblastoma-binding protein 4 (RBBP4) is an essential protein for oocyte maturation and embryo development that localizes to chromatin and functions as a small subunit of the chromatin-remodeling factor 1 (CAF-1) [22, 23]. CAF-1 assembles nucleosomes in a replication-dependent manner (Miao et al., 2020). RBBP4 loads histones H3 and H4 (specifically H3K4, H3K8, H4K12, and H4K16) onto newly

replicated DNA to institute nucleosome assembly [22, 23]. While assisting CAF-1, RBBP4 can also be called chromatin-remodeling factor RBAP48 [23].

RBBP4 localizes to chromatin and is a ubiquitously expressed nuclear protein belonging to the Trp-Asp repeating protein subunit, also known as the WD-40 family [22, 23]. Within all stages of embryo development, RBBP4 can be detected within the nucleus of the cell [23]. The localization via immunofluorescence can be seen in Figure 3. It is also found in many other protein complexes such as the histone deacetylase complex (HDAC), the nucleosome remodeling and deacetylase complex (NuRD), and the polycomb repressive complex 2 (PRC2)[24-26]. HDAC removes acetyl groups from specific amino acids on histones while NuRD and PRC2 are involved in the regulation of gene expression and lineage commitment [24, 25]. RBBP4 is a subunit in each protein complex that aids in their regulation of chromatin structure and gene transcription [23]. In addition, RBBP4 is involved in many other biological processes such as cell proliferation, apoptosis, nuclear transport, cellular senescence, DNA repair, tumorigenesis, and age-related memory loss [27-30].

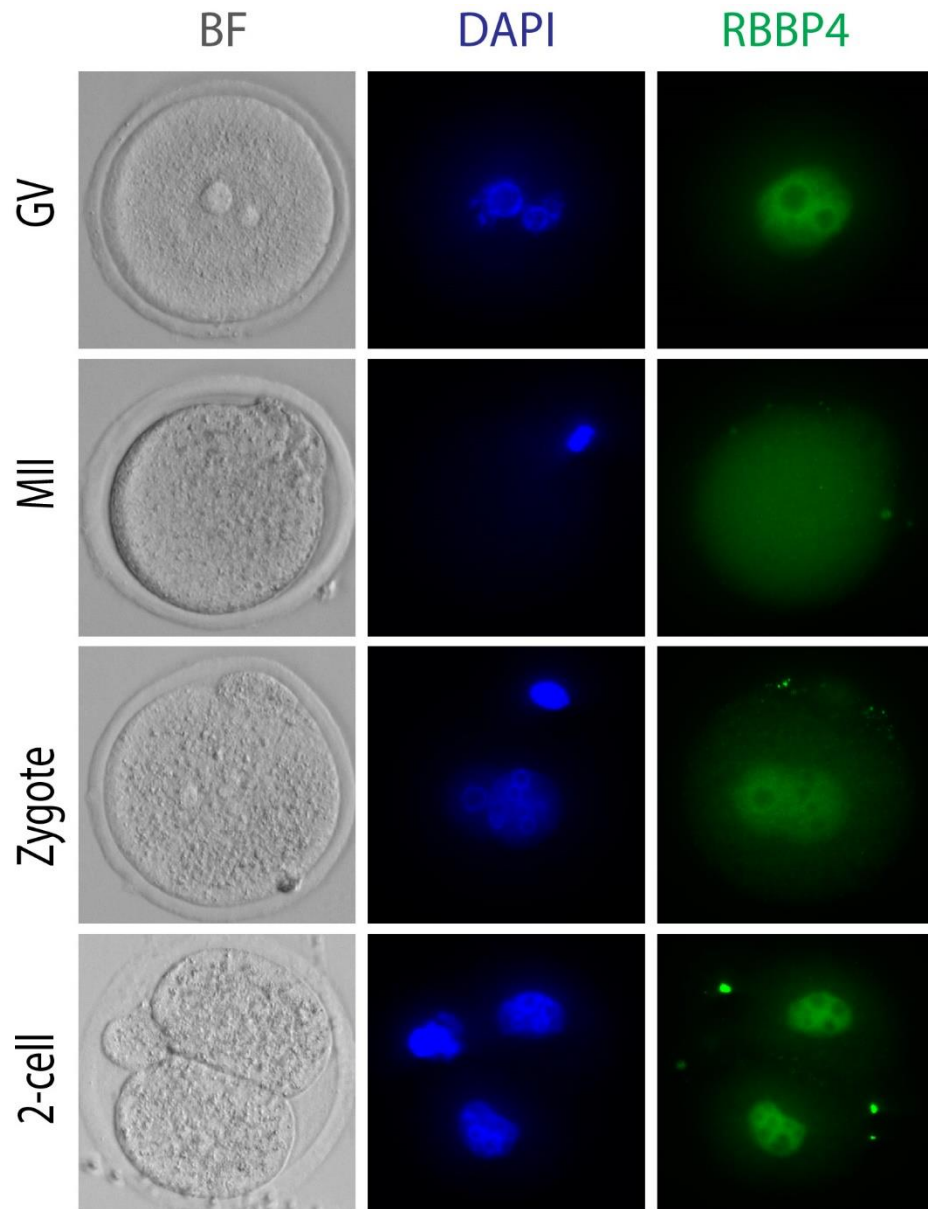


Fig 3. RBBP4 Signal from GV Oocytes to 2-cell Embryos.

IF was conducted on oocytes and embryos. There is a strong nuclear signal for RBBP4 at the GV oocyte stage, zygote embryo stage, and 2-cell embryo stage. At the MII oocyte stage RBBP4 is not detectable by IF.

During mammalian embryo development, RBBP4 is essential for proper segregation of the ICM and TE and for proper implantation. Loss of this protein within the mouse model causes reduced or absent ICM, severe apoptosis, hyperacetylated histones, and preimplantation lethality [23]. During mouse oocyte maturation, histone

deacetylation is regulated by multiple pathways. RBBP4 regulates HDACs along with retinoblastoma binding protein P46 (RBBP7), but their functions do not overlap. While these two proteins work together for successful completion of meiosis I, without the docking site for HDAC provided by RBBP4, there is abnormal bipolar spindle formation at MI with PBI extrusion defects, chromosome misalignment, and aneuploidy at MII [22]. Although great discoveries were made within both Balboula and Miao using techniques such as short interfering RNAs (siRNAs), morpholinos, and CRISPR/Cas9, each study saw limitations within their models; Balboula and colleagues could not deplete RBBP4 fully within oocytes while Miao et al., 2020 could only study their RBBP4 homozygous knockout from E4.0 to E7.5 [22, 23].

D. Trim-Away and TRIM21

Within current and past protein function studies, scientists have used methods which target the production of their target protein, including techniques such as CRISPR/Cas9 and RNA Interface (RNAi) [31]. Both methods work on the DNA or RNA level, may trigger compensatory mechanisms and may not be useful in non-dividing primary cells [32-34]. In both methods, protein depletion is indirect and dependent on the turnover of the protein, therefore long-lived proteins may take more time to deplete or may be resistant to DNA and RNA-targeting depletion [35]. There are also limitations of gene activation and loss of function phenotypes when dealing with essential genes [34]. Overall, there is a great need for a new method that will overcome these limitations by targeting the proteins directly and Trim-Away can be the answer we are looking for.

Trim-Away is a posttranslational, acute, and rapid endogenous protein depletion technique. It utilizes the tripartite motif-containing protein 21 (TRIM21)-antibody interaction within the cytosol to target a POI. When using Trim-Away, the POI does not need to be modified before degradation, proteins are degraded within minutes of application, and it allows the study of various protein functions in diverse mammalian cell types. In addition, Trim-Away is widely applicable since it can be used with many off-the-shelf reagents [35]. Trim-Away, based on the levels of target protein within the cell, TRIM21, and the amount of antibody applied, can be effective for around 3-4 days [15]. Trim-Away is about 2-12 times faster than auxin-inducible protein degradation and reduces the time of protein degradation compared to using morpholinos [12, 36].

Trim-Away requires the use of TRIM21 mRNA and a specific antibody to the POI that recognizes its native conformation [33]. The mRNA and antibody will be microinjected into a single cell or electroporation into bulk cell populations at certain time points for protein depletion to occur [35]. Microinjection, a microsurgical procedure conducted on a single cell, is a more direct approach and ensures delivery in all cells that will be treated [37, 38]. For Trim-Away to occur, the injected antibody binds to the POI and injected TRIM21 detects the antibody by binding to its fragment crystallizable region (Fc region) [39]. After all 3 of the components are bound as the protein-antibody-TRIM21 complex, it is ubiquitinated and is rapidly degraded by the proteasome [15, 35].

TRIM21 is an E3 ubiquitin ligase, multidomain, trimeric protein found in the intracellular antibody-mediated proteolysis pathway and is a type I interferon-stimulated gene [39-41]. A type I interferon is an “inducible cytosolic protein that binds to antibodies with high affinity”, can be called an antibody receptor, and substantially

upregulates TRIM21 [39, 41]. TRIM21 contains a Ring-type E3 ubiquitin ligase domain (RING domain), a B-box domain, and “a coiled-coil domain that is thought to form an antiparallel homodimer”, two of the same proteins [39, 42]. It also contains a carboxyl-terminal (C-terminal) PRYSPRY domain [39, 43]. Two copies of this domain allow for simultaneous binding of heavy chains of an antibody [39]. When the RING domain activates, it recruits the ubiquitin proteasome system to the antibody bound pathogen for the automatic creation of ubiquitin chains [39, 42, 43]. These chains have two functions: to simulate immune responses and cause proteasome-mediated destruction [39, 43].

Classical cell surface antibody receptors are very specific in isotype and subclass, unlike TRIM21. TRIM21 binds to all subclasses of Rb IgG (Rb IgG1, Rb IgG2, Rb IgG3, Rb IgG4) with similar affinities and its binding is highly conserved [39]. This means that mouse and human TRIM21 will bind to antibodies of other mammals [32]. TRIM21 is the highest Rb IgG antibody receptor in humans and can also bind to IgA and IgM, but the bond will not be as strong [39]. To use TRIM21 in an oocyte for protein depletion there is a three-step strategy written by Clift and colleagues: “first, the introduction of exogenous TRIM21; second, the introduction of an antibody against the protein of interest; and third, TRIM21-mediated ubiquitination followed by degradation of the antibody-bound protein of interest” (Figure 4) [35].

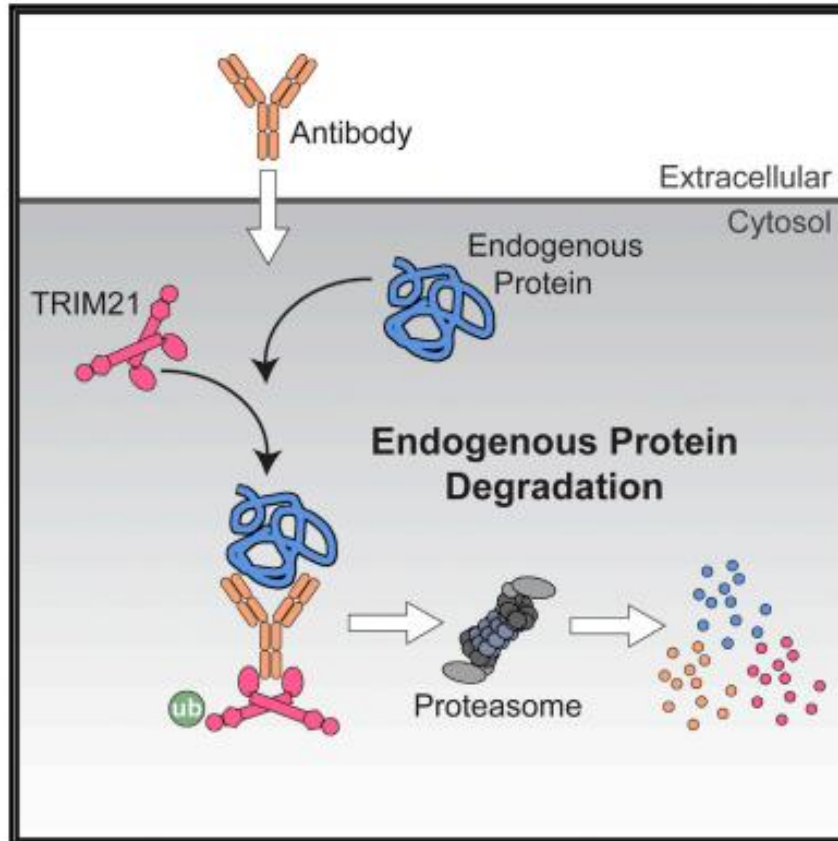


Fig 4. Trim-Away Schematic [35]

TRIM21, endogenous or overexpressed, interacts with an antibody for the degradation of an endogenous POI. The injected antibody for the POI enters the cytosol where the endogenous protein and TRIM21 reside. Once all 3 components are bound together, the POI will be tagged with a ubiquitin chain which then will be dragged to the proteasome where it will be subsequently degraded.

E. Aim of Study

Based on previous studies, we know RBBP4 is essential for mammalian oocyte maturation, embryo survival, and embryo implantation. These studies used genetic techniques such as short interfering RNAs (siRNAs), morpholinos, and CRISPR/Cas9, which provided limitations within their experiments. Miao et al., 2020 was conducted through a collaboration between the Mager lab and our lab, by using a knockout RBBP4 mouse model. The limitation we saw was breeding a heterozygous female with

heterozygous males. Maternally loaded RBBP4 was present within these knockout embryos and was not degraded until after flushing embryos from the uterine horns and culturing overnight to E4.0. Having a knockout (mutant) sperm fertilize a mutant oocyte for a homozygous knockout, caused embryo lethality after E7.5 and the later depletion of Rbbp4 did not allow for early embryo development to be studied in-depth. In additions, MEGs were not explored during Miao's study. Since the Rbbp4 gene is highly expressed during oogenesis and oocyte maturation, we wanted to extend our studies to define the role of RBBP4 within oocyte maturation and early embryo development. Within this current study, we will be using Trim-Away for the rapid depletion of RBBP4 to study its effects on oocyte maturation and early embryo development. Studying RBBP4 using Trim-Away can offer insight into possible new functions of RBBP4 and its maternal effect, and increase the knowledge on a new, acute, and endogenous protein depletion technique.

CHAPTER 2

MATERIALS AND METHODS

A. Ethics statement and animal use

C57BL/6 RBBP4 wildtype (WT) mice were used for all experimental procedures and methods approved by the Institutional Animal Care and Use Committee of the University of Massachusetts Amherst (2017- 0071). All mice were maintained on provided water ad libitum under a 12-hour (h) light: dark cycle. Proper training was obtained for euthanasia of mice using the approved method of cervical dislocation via Dr. J. Paul Spurlock, Director of Animal Care and Attending Veterinarian at the University of Massachusetts Amherst.

B. Oocyte and zygote collection

Fully grown GV oocytes were collected from 6–8-week-old female mice that were injected intraperitoneally (IP) with 0.3 mL of pregnant mares' serum gonadotropin (PMSG) 45-46h previously. Ovaries were removed and placed into a 1X cilostamide (Cat#C7971-5MG) solution containing EmbryoMax M2 Medium with Phenol Red (Millipore, MR-015-D) for cell cycle arrest. Antral follicles were punctured using a sterile 26-gauge, 1 mL needle and the oocytes were collected for cumulus cell removal. The cumulus cells were removed with a pulled 1.0mm OD tip from Fisher Scientific.

Mature ovulated MII oocytes were collected from 6–8-week-old female mice that were injected IP with 0.3 mL of human chorionic gonadotropin (hCG) 48h after PMSG treatment. Ovaries and oviducts were removed 18h and placed into M2 medium. MII arrested oocytes were collected from the ampulla of the oviduct and placed into

EmbryoMax M2 Medium with Hyaluronidase (Millipore, MR-051-F) for 3-5 minutes. Cumulus cells were removed with a pulled and fire polished 1.5mm OD tip.

Zygotes were collected from 6–8-week-old female mice that were injected IP with 0.3 mL of hCG and directly mated with double studs 48h after PMSG treatment. Ovaries and oviducts were removed 18h later and placed into M2 medium. Zygotes were collected from the ampulla of the oviduct and placed into M2 Medium with Hyaluronidase for 5 minutes. Cumulus cells were removed with a pulled and fire polished 1.5mm OD tip.

C. mRNA preparation

All plasmids used to generate mRNA were purchased from Addgene and include pGEMHE-mEGFP-mTRIM21, pGEMHE-mCherry-mTRIM21, pGEMHE-H2B-mEGFP, and pGEMHE-mEGFP-Map4 [44]. Each plasmid was streaked on an LB agar plate for overnight culture in 37°C incubator using sterile inoculating loops. The next morning, single colonies were collected for liquid culture in LB with ampicillin overnight in an incubating minishaker at 37°C. Plasmids were isolated the following afternoon using a QIAprep Spin Miniprep Kit (Qiagen, 27104). Each plasmid was validated by cutting the plasmid twice with buffers and enzymes from New England BioLabs [45]. Buffers and enzymes used include CutSmart Buffer (NEB, B7204S), 3.1 Buffer (NEB, B7203S), AscI enzyme (NEB, R0558S), EcoRI enzyme (NEB, R0101S), HindIII enzyme (NEB, R0104S), SwaI enzyme (NEB, R0604S), and AgeI enzyme (NEB, R0552S). A 1% agarose gel was run to confirm these cuts. All agarose gels contain Ethidium Bromide (Millipore-Sigma, 1239-45-8) for DNA and RNA detection, unless otherwise stated. The enzyme used to cut each respective plasmid can be found in Table 1. After validation, the

plasmids were linearized. Capped mRNA was then synthesized through *in vitro* transcription via a mMESAGE mMACHINE T7 Kit (Invitrogen, AM1344). Enzymes AscI and SwaI were used for linearization. A 1% agarose gel was run to confirm the linearization. The enzymes used for each respective plasmid can be found in Table 2. All plasmids were then purified using a Phenol: Chloroform protocol from ThermoFisher Scientific using UltraPure Phenol: Chloroform: Isoamyl Alcohol (ThermoFisher, 15593031). Lastly, all RNA was purified using ethanol precipitation through a MEGAclear Transcription Clean-Up Kit (Invitrogen AM1908). The purified RNA was diluted using a ratio of either 0.2 μ L RNA: 3 μ L nuclease free water or 0.2 μ L RNA: 5 μ L nuclease free water. Concentrations for each RNA extraction were measured on a spectrophotometer. A 1% agarose gel was run to confirm all purifications. All plasmids used and protocols followed were similar to those from Clift et al., 2017.

mRNA	Buffer	Enzyme
pGEMHE-mEGFP-mTRIM21	CutSmart	AscI EcoRI
pGEMHE-mCherry-mTRIM21	CutSmart	AscI EcoRI
pGEMHE-H2B-mEGFP	3.1	HindIII SwaI
pGEMHE-mEGFP-Map4	CutSmart	AscI AgeI

Table 1. Plasmid Validation Buffers and Enzymes

AscI cuts the plasmid at 787 bp. EcoRI cuts the plasmid at 1546 bp. HindIII cuts the plasmid at 1021 bp. SwaI cuts the plasmid at 2209 bp. AgeI cuts the plasmid at 5222 bp.

mRNA	Buffer	Enzyme
pGEMHE-mEGFP-mTRIM21	CutSmart	AscI
pGEMHE-mCherry-mTRIM21	CutSmart	AscI
pGEMHE-H2B-mEGFP	3.1	SwaI
pGEMHE-mEGFP-Map4	CutSmart	AscI

Table 2. Plasmid Linearization Buffers and Enzymes

AscI cuts the plasmid at 787 bp. SwaI cuts the plasmid at 2209 bp.

D. Microinjection

All microinjections were conducted using a Nikon Eclipse Ts2R microscope, Eppendorf *PiezoXpert*, and an Eppendorf *TransferMan 4r*. All GV oocytes were arrested with cilostamide until cell cycle release after all microinjections were completed. All injected mRNA and antibody concentrations are listed in Table 3. mRNA was injected for freshly collected oocytes and zygotes and incubated for 1-3h for overexpression of mRNA injected, in 37 °C in a humidified atmosphere of 5% CO₂, 5% O₂ balanced in N₂. Additionally, GV oocytes were cultured in KSOM with castanoside for 1h to allow for a larger perivitelline space. After the allotted culture times, the desired antibody was injected into the same cells. Only GV oocytes were treated with cytochalasin B (CB) right before microinjection of antibodies. All cells were live imaged for confirmation of TRIM21 mRNA injection success. When antibodies were purified, an Amicon Ultra 0.5mL 100K kit (Millipore, UFC510008), diluted in Dulbecco's Phosphate Buffered

Saline (DPBS) (Gibco, 14190-1440) was used. Both unpurified and purified antibodies are stated in each figure where antibodies were used, and antibody purification concentrations are listed in Table 3. Figure 5 represents the microinjection technique used for all mRNA and antibody injections.

mRNA	Concentration (ng/ μ L)	Antibody	Concentration (mg/mL)
pGEMHE-mEGFP-mTRIM21	750 or 300	Anti-RBBP4	Unpurified: 0.11 Purified: 0.35
pGEMHE-mCherry-mTRIM21	300	Anti-GFP	0.35
pGEMHE-H2B-mEGFP	200	Anti-H2B	1.1
pGEMHE-mEGFP-Map4	300	Anti-MAP4	0.8
-	-	Rb IgG	0.35

Table 3. mRNA and Antibody Microinjection Concentrations

Where there are 2 concentrations of mRNA listed, the second number is the optimized concentration. The mRNA and antibody listed within the same row, do not correlate with injection days or to each other. Each mRNA injection was paired with a different antibody for injection based on the daily experimental plan.

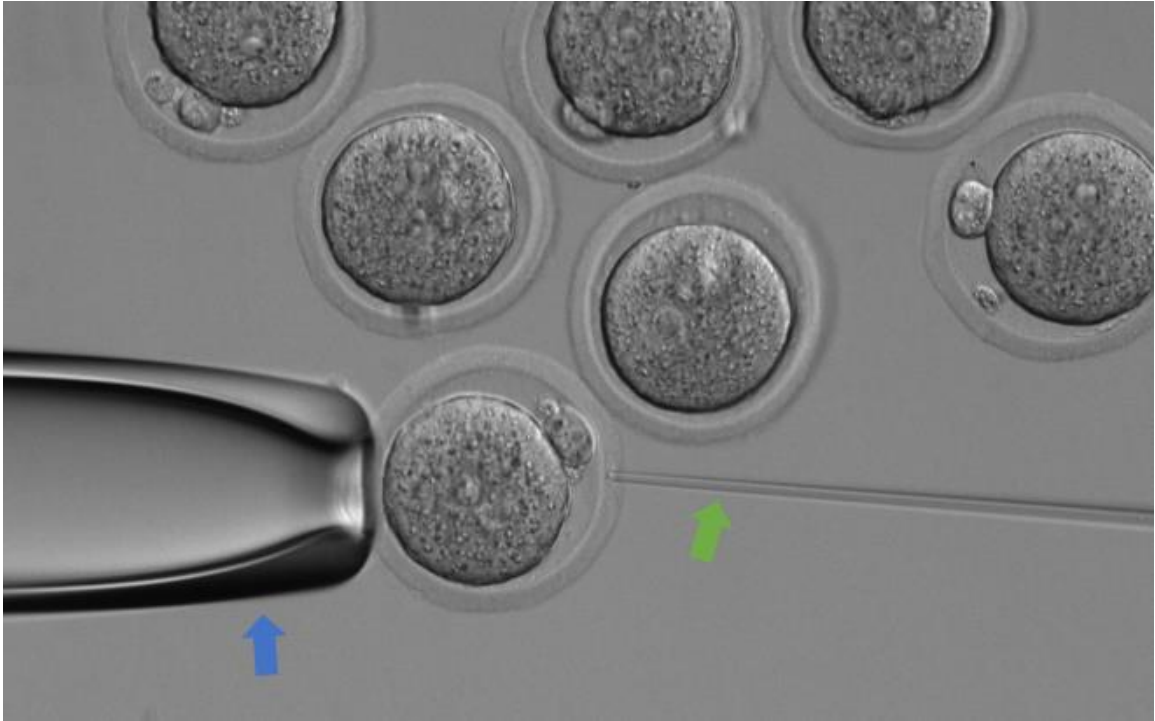


Fig 5. Microinjection of Zygote

Before injection of TRIM21 mRNA and antibody, the CellTram 4r Air controlled holding pipette (blue arrow) contacts the oocyte or embryo and stabilizes it. Once the cell is in place, the injection needle will pierce the zona pellucida (ZP) and cytoplasm for injection of TRIM21 mRNA and antibody. The injection needle, controlled by the CellTram 4r Oil microinjector, releases the desired contents into the cell [45].

E. Immunofluorescence (IF)

Oocytes and zygotes were fixed in 4% paraformaldehyde (PFA) either for 20 minutes at room temperature or overnight in 4 °C and washed in 24 well plate for 10 minutes at 100 RPM on a Boekel Flask Dancer in PBS/10% FBS. The cells were then permeabilized for 20 minutes in a solution containing PBS/0.3%PVP/0.5% Triton and moved to a blocking solution containing PBS/10% FBS/0.1% Triton for 1h. The cells were incubated in the appropriate primary antibody for either 1h room temperature or overnight in 4 °C. All primary antibodies except anti-MAP4 were diluted at a ratio of 1:200 antibody: block including rabbit anti-RBBP4 (Abcam, ab79416), mouse anti-H2B

(Abcam, ab52484), rabbit anti-Histone4K5 + K8 + K12 + K16 (Abcam, ab10807). Rabbit anti-MAP4 (Millipore-Sigma AB6020) was diluted at a ratio of 1:1000. After washing the cells in a 24 well plate for 10 minutes at 100 RPM on a Boekel Flask Dancer in block solution, the appropriate secondary antibody (Alexa Fluor, Thermo Fisher Scientific, Waltham, MA, USA) was applied with a ratio of 1:500 antibody: block for 1h. After another wash, cells were stained for DNA with DAPI diluted with PBS/10% FBS for 20 minutes. After washing with PBS/10%FBS, cells were mounted on microscope slides and imaged using a Nikon Eclipse Ts2R microscope.

F. Live imaging

Oocytes and zygotes were transferred to M2 medium, EmbryoMax KSOM+AA with D-Glucose culture medium (Millipore, MR-106-D) covered with EmbryoMax Light Mineral Oil (Millipore, ES-005-C) and imaged using a Nikon Eclipse Ts2R microscope. All live imaging was performed after antibody injection using a 60mm culture dish. Images were taken at different time intervals based on developmental stage of oocyte or embryo (see respective figures for exact time intervals).

G. *In vitro* maturation (IVM) of oocytes

GV oocytes were collected as mentioned above and were arrested with cilostamide until cell cycle release after all microinjections were completed. GV oocytes were washed in M2 medium without cilostamide and KSOM without cilostamide. Finally, the oocytes were cultured overnight in KSOM without cilostamide, to the MII stage. Live images were taken at 1h after microinjection and the following morning for TRIM21-mCherry mRNA confirmation. These samples were then used for western blot.

H. Western blot

MII oocytes from in vitro maturation or from a fresh collection and were transferred into 5-8 μ L of PBS/10% Sample Buffer 2 (lysis buffer) (ProteinSimple, 042-195), vortexed and centrifuged. Mouse liver serving as a positive control for RBBP4 was dissolved in 5 μ L of PBS/10% Sample Buffer 2, vortexed, and centrifuged. Samples were brought to the Alfandari lab (University of Massachusetts Amherst) to run a western blot analysis using the Wes machine, which automates traditional western blotting. Anti-RBBP4 was used to detect if RBBP4 protein was present in MII oocytes while anti-GAPDH was used as a control to detect GAPDH, a housekeeping gene that will be present in all samples. Both antibodies were diluted 1:100 in antibody diluent solution (Protein Simple, 042-203). An EZ Standard Pack 1 (Protein Simple, PS-ST01EZ) was used to prepare the separation module. 40 μ L of deionized water was added to the DTT tube to make a 400mM solution. 20 μ L of 10X Samples Buffer 2 and 20 μ L of the previously prepared 400mM DTT solution was added to the 5X Fluorescent Master Mix. 20 μ L of deionized water was added to the Biotinylated Ladder tube. The secondary HRP conjugate used were rabbit for RBBP4 and mouse for GAPDH, respectively. The secondary HRP conjugate for rabbit was diluted as 1:50 since it was previously diluted with glycerol. To achieve 1-part 5X Fluorescent Master Mix: 4-parts sample, 2 μ L of 5X Fluorescent Master Mix was added to the 8 μ L of M2 oocyte sample and 1.2 μ L of 5X Fluorescent Master Mix was added to the 5 μ L of live sample. All samples were denatured at 95 $^{\circ}$ C for 5 minutes and stored on ice until used. 200 μ L of Luminol-S and 200 μ L of peroxide (ETC) were combined in a microcentrifuge tube and stored on ice until use. The top half of the microplate (Cat# SM-W004) was peeled off while leaving

the bottom half intact until run time, due to an evaporative gel material. Samples and other solutions were loaded into the microplate according to Figure 6 and centrifuged for 5 minutes at 1000 x g at room temperature. After separating proteins by molecular weight, the proteins were immobilized via UV light in a glass capillary tube. They were incubated with the respective primary antibody and respective secondary HRP conjugate. The chemiluminescence of each sample was quantified by using the ETC. Normal Wes run time is about 2-3 hours.

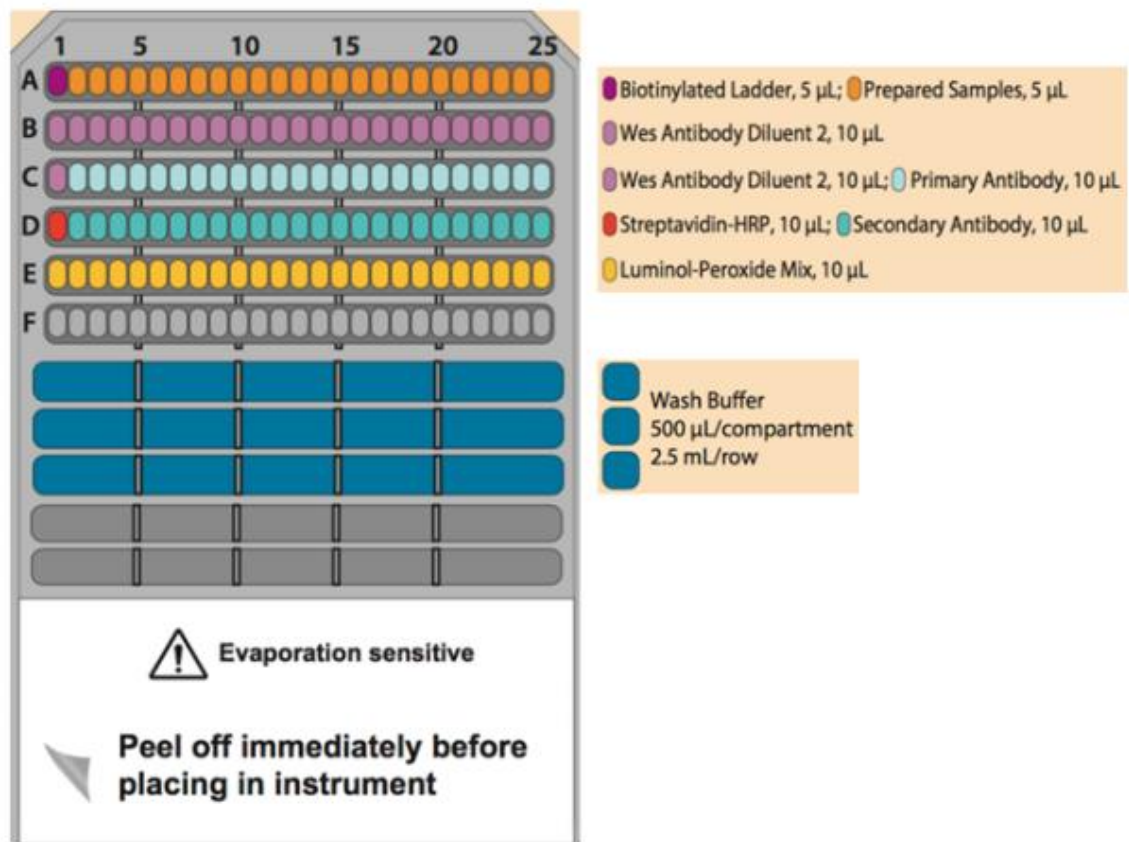


Fig 6. Wes Microplate Loading Schematic

Each reagent and prepared sample will be aliquoted into the appropriate well for automatic loading into glass capillaries within the Wes machine. The bottom seal should be peeled off directly prior to loading the microplate into the machine due to evaporative materials.

I. 5-ethynyl uridine (EU) incorporation assay

The Click-iT RNA Alexa Flour 488 Imaging Kit used (ThermoFisher, C10329) was used to detect nascent (newly synthesized) RNA temporally and spatially in embryos. This kit was aliquoted in house before use. KSOM medium with 100 μ M EU was equilibrated for 2h in 37 °C in a humidified atmosphere of 5% CO₂, 5% O₂ balanced in N₂. Embryos were then cultured in the same KSOM medium for an additional 2h under the same conditions for the alkyne-containing nucleoside (EU) to be incorporated into nascent RNA. Embryos were then immediately fixed, permeabilized, and stained with either DAPI or with the appropriate primary and secondary antibody, according to the manufacturer's protocols. DAPI was diluted with PBS/3% PVP and embryos were washed afterwards using PBS/3% PVP as well. Embryos were then mounted on microscope slides and imaged using a Nikon Eclipse Ts2R microscope.

J. Terminal deoxynucleotidyl transferase dUTP nick end labeling (TUNEL)

Terminal deoxynucleotidyl transferase dUTP nick end labeling (TUNEL) staining was performed using the In Situ Cell Death Detection Kit (Roche, 11684795910) as a DNA break assay, according to the manufacturer's protocol. Embryos were collected, fixed, and permeabilized as mentioned above. After permeabilization, embryos were washed in a 24 well plate for 10 minutes at 100 RPM on a Boekel Flask Dancer in PBS/10% FBS. Embryos were moved into the TUNEL reaction mixture containing a 1:10 mixture of Enzyme Solution (TdT) (Roche, 11684795910) and Label Solution (fluorescein-dUTP) (Roche 11684795910), protected from light for 30 minutes at 37°C. After washing, embryos were stained with DAPI and washed once more. Embryos were then mounted on microscope slides and imaged using a Nikon Eclipse Ts2R microscope.

CHAPTER 3

RESULTS

A. Generation of mRNA

mRNA which would then be injected into the oocyte or embryo was generated using the different plasmids listed in Table 1. To validate and linearize the plasmids a 1% agarose gel was run (not shown) for confirmation. After each RNA purification, another 1% agarose gel was run for confirmation (Figure 7). Figure 7A and Figure 7B gels show the RNA present within the diluted sample at different points in the plasmid and RNA purification processes. The concentration was also measured via a spectrophotometer and considered when choosing mRNA to inject. Comparing the concentration of RNA after purification in Figure 7A, plasmid #3 (P3) with no Phenol: Chloroform purification decreased to 19% RNA present, while the Phenol: Chloroform purified P3 decreased to 16% RNA present. Additionally, in Figure 7B the Phenol: Chloroform purified plasmid #1 (P1) decreased to 13% RNA present and 24% after RNA Purification. Without some form of plasmid purification, successful RNA purification was not consistent in providing high concentrations, which can be observed from multiple RNA purification experiments previously conducted within the lab (not shown).

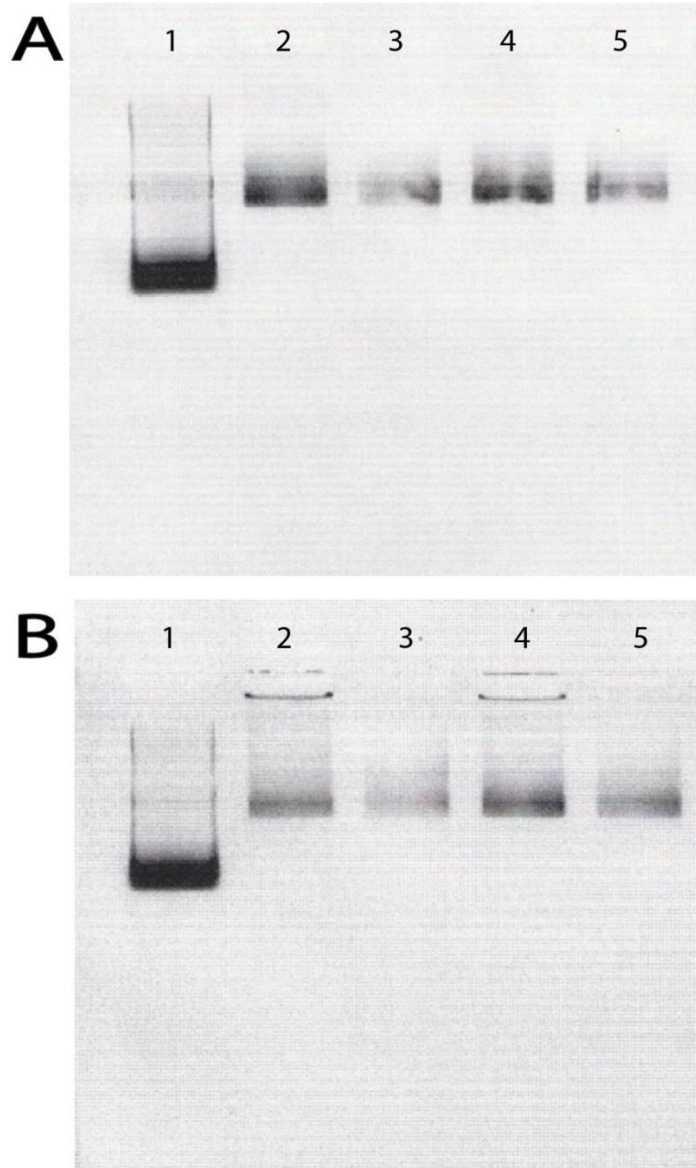


Fig 7. pGEMHE-mEGFP-mTRIM21 and pGEMHE-mCherry-mTRIM21 RNA Purification

A.) This RNA purification was done with isolated P3 Lane 1 represents the 1KB ladder. Lane 2 represents the total RNA after in vitro transcription, but before RNA purification (8290 ng/ μ L). Lane 3 represents the total RNA after IVT and RNA purification (1640 ng/ μ L). Lane 4 represents the total RNA after in vitro transcription and plasmid Phenol: Chloroform purification, but before RNA purification (9940 ng/ μ L). Lane 5 represents the total RNA after IVT, Phenol: Chloroform plasmid purification and RNA purification (1670 ng/ μ L). B.) This RNA purification was done with isolated P1. Lane 1 represents the 1KB ladder. Lane 2 represents the total RNA after in vitro transcription, but before RNA purification (8500 ng/ μ L). Lane 3 represents the total RNA after IVT, Phenol: Chloroform plasmid purification, and RNA purification (1140 ng/ μ L). Lane 4 represents the total RNA after in vitro transcription and plasmid Phenol: Chloroform purification (6150 ng/ μ L), but before RNA purification. Lane 5 represents the total RNA after IVT, Phenol/Chloroform plasmid purification and RNA purification (1520 ng/ μ L).

B. Trim-Away Methodology Confirmation

All injected antibodies were purified unless otherwise stated. We first injected TRIM21-mEGFP mRNA for overexpression and anti-RBBP4 (unpurified) simultaneously into GV oocytes (Figure 8). After fixation and immunofluorescence, it was clear that TRIM21-mEGFP was not overexpressed within these oocytes and consequently, the RBBP4 protein was not depleted from the nucleus. Unsure as to the cause of this (RNA or antibody related) we wanted to test the quality of our RNA. We conducted separate injections of mRNA and antibody (Figure 9). GV oocytes were injected with TRIM21-mEGFP mRNA and after a waiting period of 3h, anti-RBBP4 (unpurified) was injected. After fixation and immunofluorescence, TRIM21-mEGFP was overexpressed, but the RBBP4 protein was still not depleted from the nucleus. These results show there was no significant difference between the negative control (un-injected) and the anti-RBBP4 injected GV oocytes and that our mRNA quality is optimal for Trim-Away methodology.

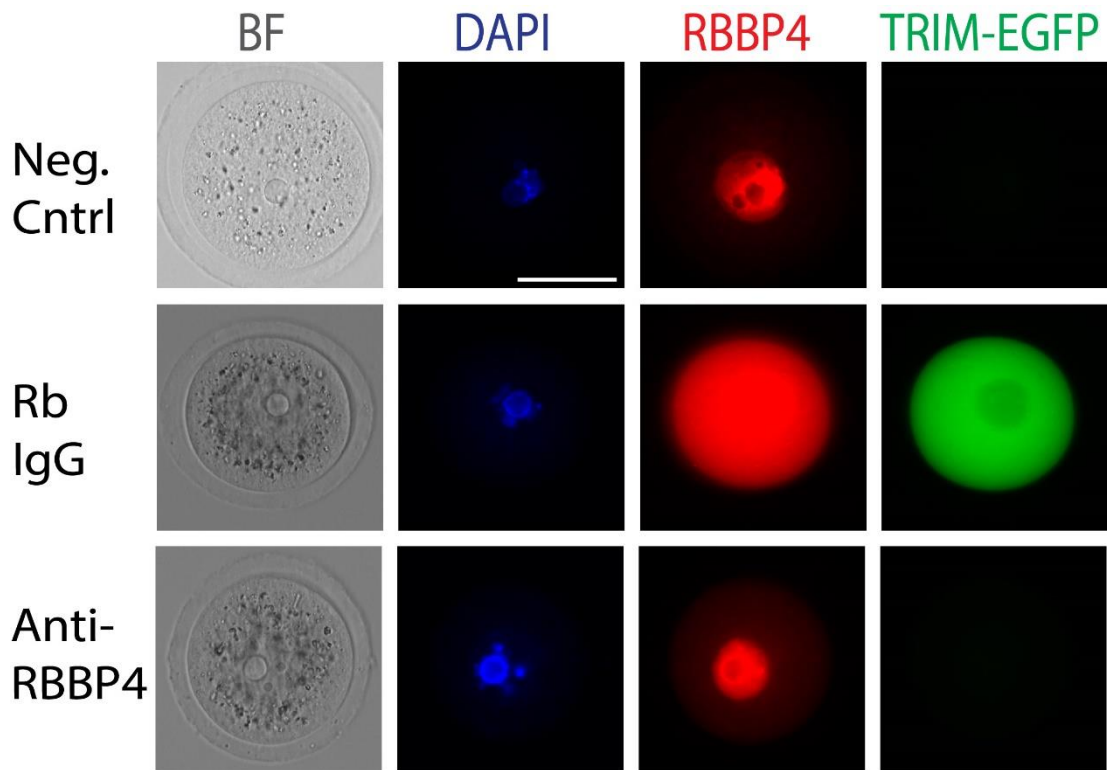


Fig 8. Co-injection of TRIM21 mRNA and Anti-RBBP4 in GV Oocytes
 3 hours after a co-injection of pGEMHE-mEGFP-mTRIM21 and anti-RBBP4, GV oocytes were fixed. Immunofluorescence was conducted to observe the concentration of TRIM21 mRNA and RBBP4 protein present. Anti-RBBP4 was not purified.

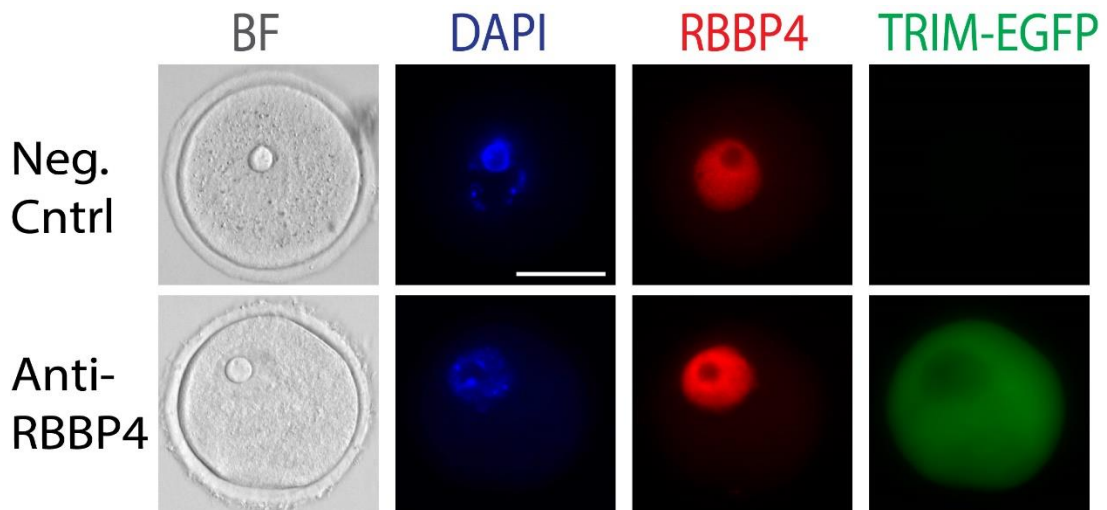


Fig 9. Separate Injections of TRIM21 mRNA and Anti-RBBP4 in GV Oocytes
 Anti-RBBP4 was injected 3 hours after injection of mRNA from pGEMHE-mEGFP-mTRIM21. GV oocytes were incubated at 37°C for 3 hours and then fixed. Immunofluorescence was conducted to observe the concentration of TRIM21 mRNA and RBBP4 protein present. Anti-RBBP4 was not purified.

To test our Trim-Away methodology, we chose to look at 2 different proteins at the MII oocyte stage, H2B and MAP4. We first looked at H2B. H2B was overexpressed with H2B-mEGFP mRNA along with TRIM21-mCherry overexpression 3h before anti-H2B (unpurified) was injected (Figure 10). These oocytes were live imaged for 120 minutes after antibody injections. There was a depletion of H2B protein and TRIM21-mCherry at 30 minutes. After 30 minutes the H2B protein and TRIM21-mCherry expression returned. To see if the H2B protein could be trimmed away if allotted a longer culture time, we repeated the previously mentioned experiment of overexpressing H2B with H2B-mEGFP mRNA along with TRIM21-mCherry overexpression 3h before anti-H2B was injected (Figure 11). We saw that at 40 minutes, the H2B protein was depleted once again, but when these MII oocytes were incubated overnight, the H2B protein and TRIM21-mCherry signal returned with an even stronger concentration than there was previously at the 40-minute mark. In addition, we conducted Trim-Away using TRIM21-mCherry anti-H2B in zygotes and at each allotted time a live image was taken (Figure 12). During the zygote and 2-cell stage, there was little to no depletion seen in anti-H2B injected embryos.

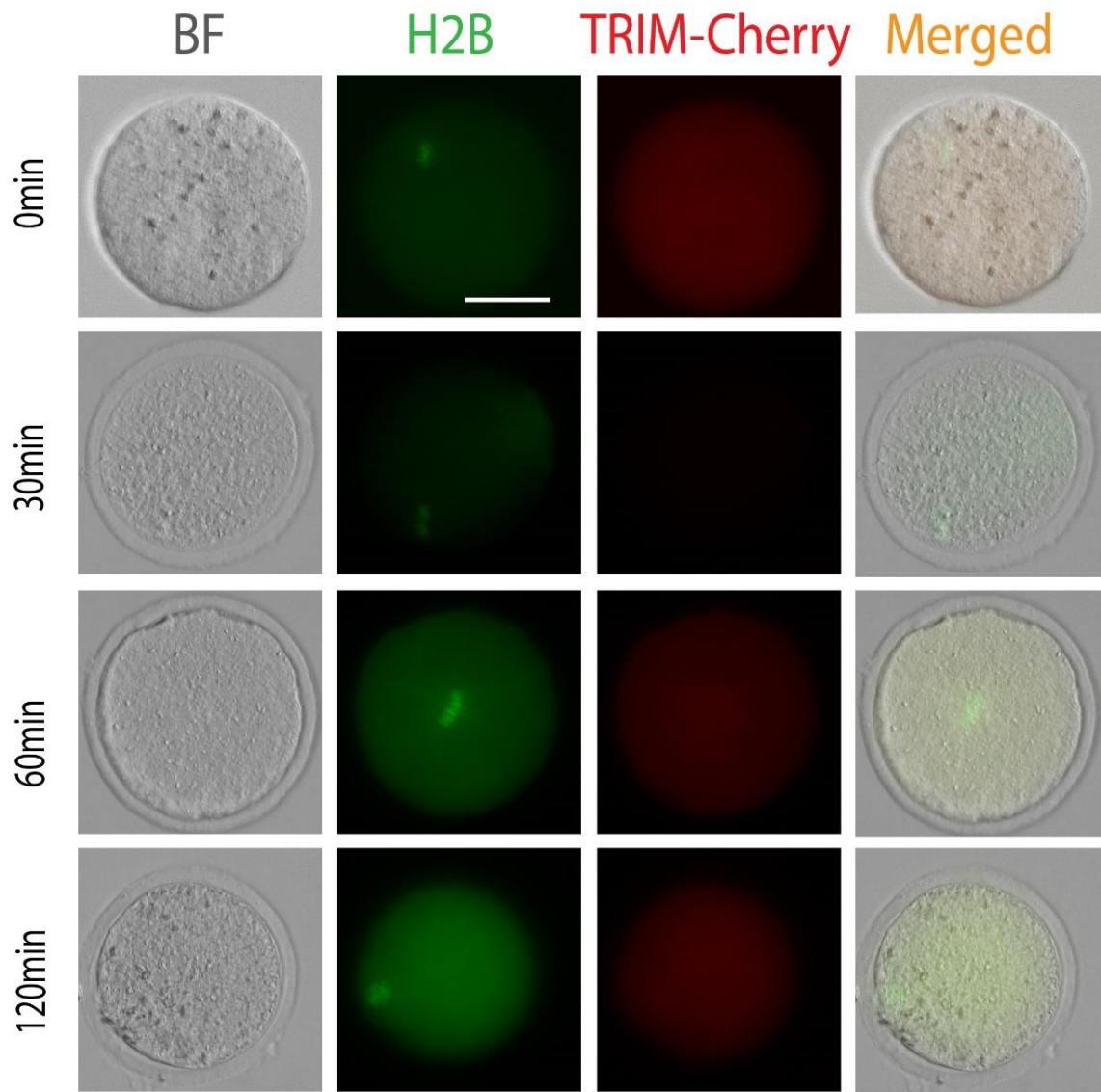


Fig 10. Trim Away of H2B Using Unpurified Anti-H2B in MII Oocytes

Anti-H2B was injected 3 hours after injection of mRNA from pGEMHE-mEGFP-mTRIM21 and H2B-mEGFP. MII oocytes were live imaged to observe the concentration of TRIM21 mRNA and H2B protein present. There was a depletion of H2B protein at 30 minutes. Anti-H2B was not purified.

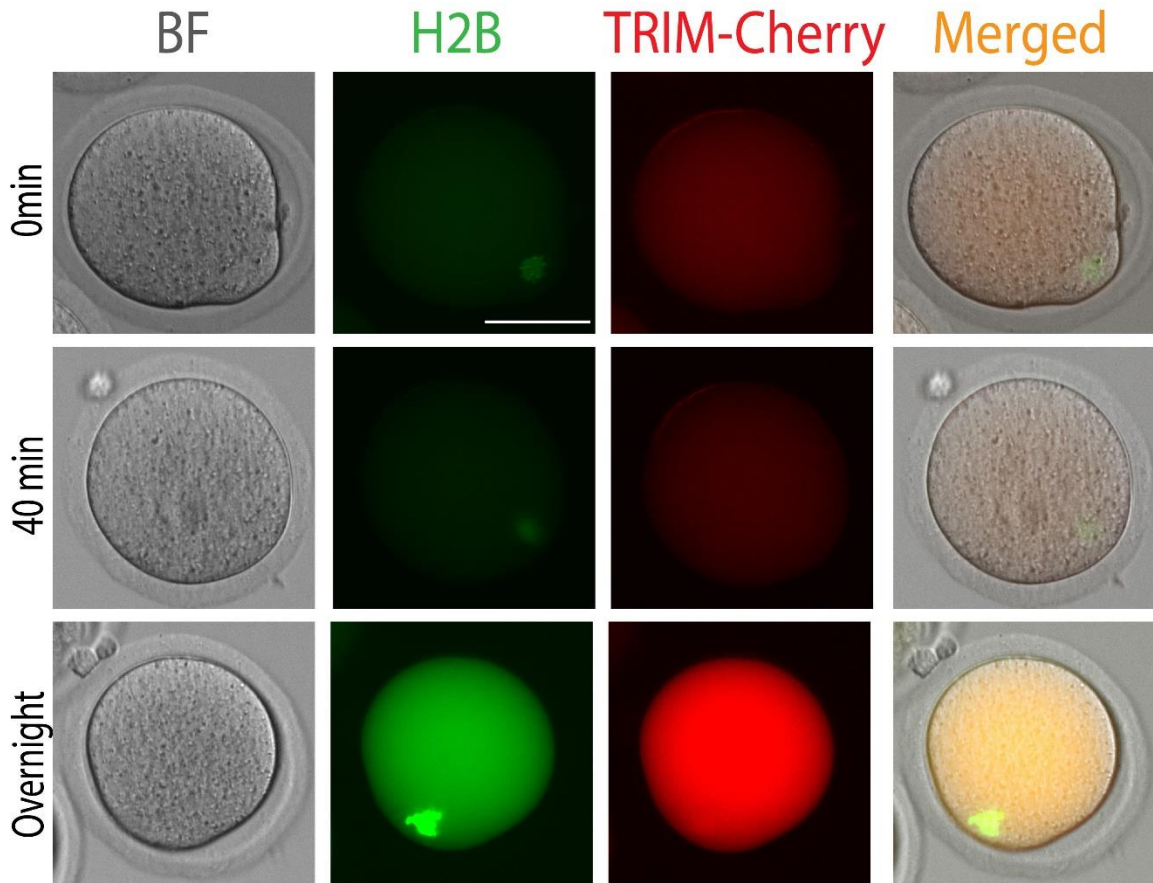


Fig 11. Trim Away of H2B Using Purified Anti-H2B in MII Oocytes

Anti-H2B was injected 3 hours after injection of mRNA from pGEMHE-mEGFP-mTRIM21 and H2B-mEGFP. MII oocytes were live imaged to observe the concentration of TRIM21 mRNA and H2B protein present. There was a depletion of H2B protein at 40 minutes. Anti-H2B was purified.

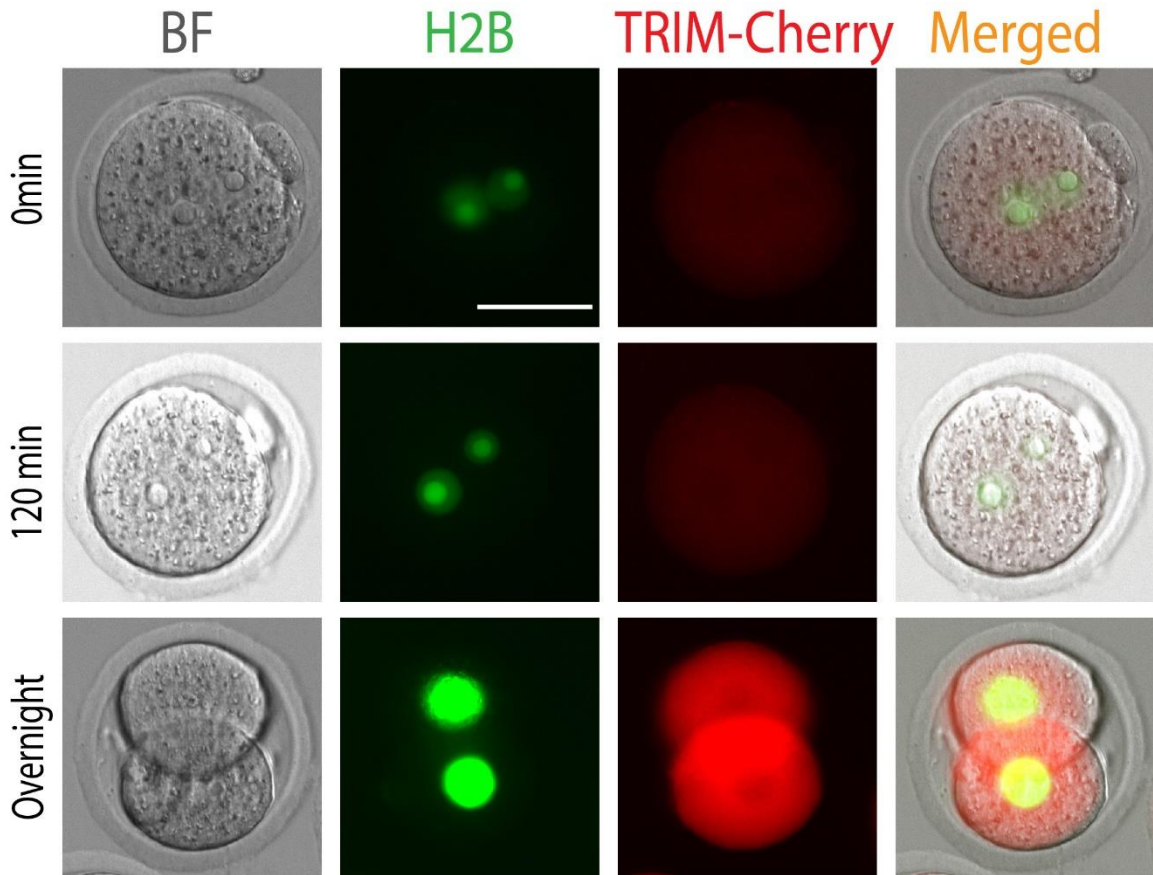


Fig 12. Trim Away of H2B Using Purified Anti-H2B in Zygotes and 2-cell Embryos
 Anti-H2B was injected 3 hours after injection of mRNA from pGEMHE-mEGFP-mTRIM21 and H2B-mEGFP. Zygotes and 2-cell embryos were fixed, and immunofluorescence was conducted to observe the concentration of TRIM21 mRNA and H2B protein present. little to no depletion was seen using Anti-H2B in zygotes or 2-cell embryos. Anti-H2B was purified.

Taking another look at the original Trim-Away paper from Clift and colleagues, while overexpressing H2B and MAP4, they rabbit anti-GFP (Abcam, ab6556) as their antibody of choice against both proteins [35]. When we compared injecting anti-H2B to injecting anti-GFP 3h after H2B-mEGFP and TRIM21-mCherry overexpression, there was a significant difference in the long-term depletion of the H2B protein (Figure 13).

We also focused on MAP4 protein and TRIM21-mCherry overexpression (Figure 14). MAP4 overexpression was conducted using MAP4-mEGFP mRNA. At the 10-minute and 80-minute mark, there was little to no difference between each group. This was most likely due to low MAP4 mRNA concentrations. We allowed these oocytes to incubate overnight for a clearer conclusion if Trim-Away occurred. With the overnight incubation, the anti-GFP and anti-MAP4 group had clear depletions of MAP4 protein compared to the RNA Only and Rb IgG injected groups. These results suggest that anti-Map4 was sufficient in depleting the MAP4 protein, but anti-GFP was optimal for a greater depletion and for providing longer lasting results for both H2B and Map4 protein depletion.

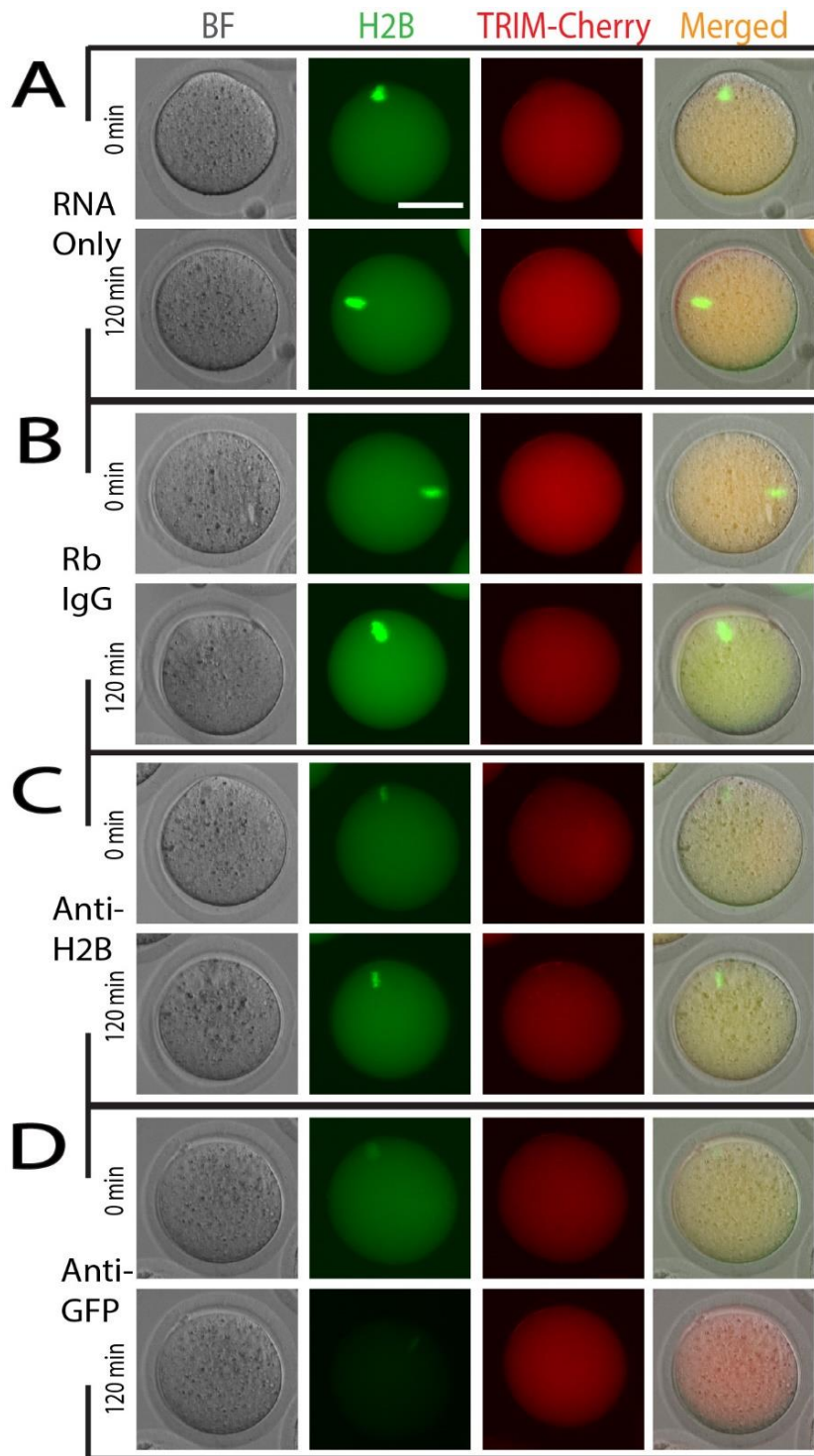


Fig 13. Trim Away of H2B Using Purified Anti-H2B and Purified Anti-GFP

Either Anti-H2B or Anti-GFP was injected 3 hours after injection of mRNA from pGEMHE-mEGFP-mTRIM21 and H2B-mEGFP. MII Oocytes were live imaged to observe the concentration of TRIM21 mRNA and H2B protein present. There was a depletion of H2B protein at 120 minutes using Anti-H2B. Anti H2B and Anti-GFP were purified.

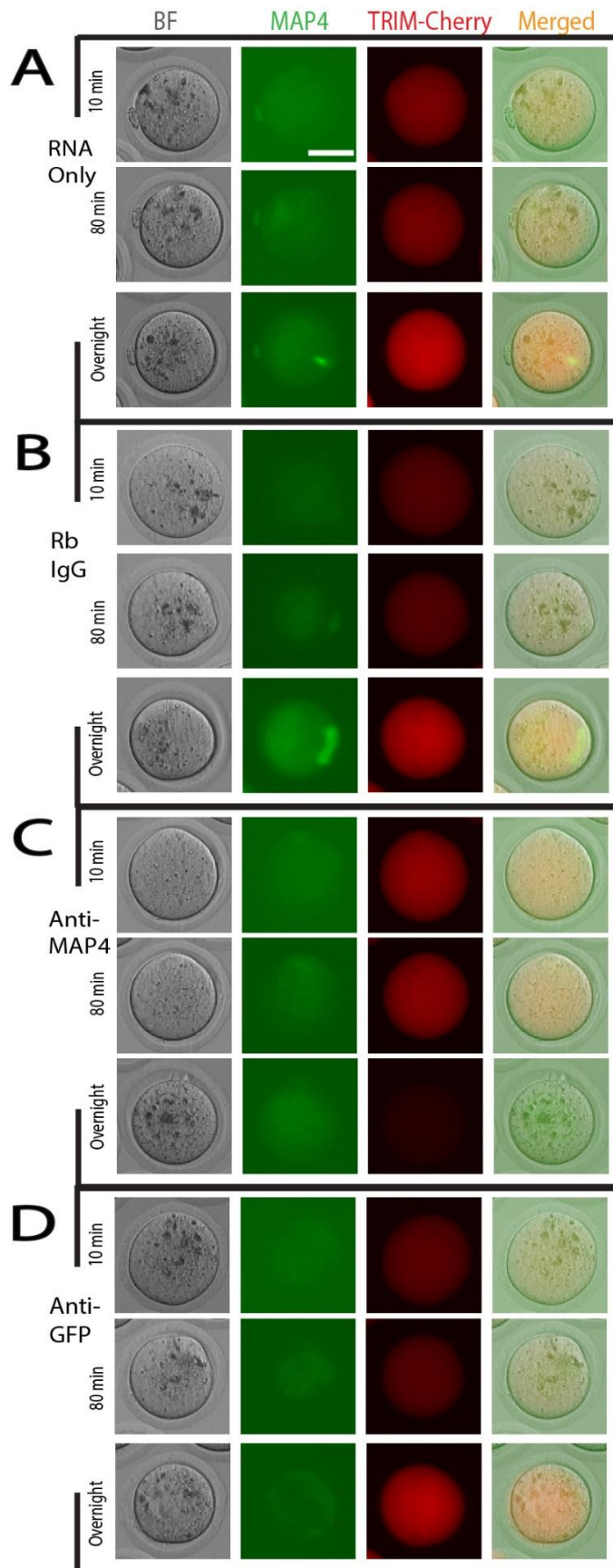


Fig 14. Trim-Away of MAP4 Using Purified Anti-MAP4 and Purified Anti-GFP

Either Anti-MAP4 or Anti-GFP was injected 3 hours after injection of mRNA from pGEMHE-mEGFP-mTRIM21 and MAP4-mEGFP MII Oocytes were live imaged to observe the concentration of TRIM21 mRNA and MAP4 protein present. There was a depletion of MAP4 protein at 80 minutes using both Anti-MAP4 and Anti-GFP. There was long lasting depletion when injecting either Anti-Map4 or Anti-GFP, but GFP had more depletion overall. Anti-MAP4 and Anti-GFP were purified.

C. Trim-Away in Embryos

Since our methodology was confirmed, we moved forward and focused on our target protein, RBBP4. Continuing to use TRIM21-mCherry overexpression, we then injected anti-RBBP4 into zygotes 3h later. The zygotes were cultured for 3h or overnight for development into 2-cell embryos (Figure 15A). Anti-RBBP4 injected zygotes cultured 3h after their antibody injection had no depletion of RBBP4. There was a clear nuclear signal for RBBP4 still present. Zygotes that were cultured until the 2-cell stage had a no nuclear signal for RBBP4 within the nucleus (Figure 15B).

The antibody used for the Rb IgG control embryos was not purified for this experiment. The cytoplasm within the RNA Only injected embryos, Rb IgG injected embryos, and anti-RBBP4 injected embryos, had a higher cytoplasmic signal than the nothing control (un-injected) embryos. This is because both injected antibody (Rb IgG or Rb Anti-RBBP4) and TRIM21 can both bind to the secondary anti-rabbit antibody during IF.

This RBBP depletion from the 2-cell stage lasted through 4 and 8-cell embryos (Figure 15C and 15D), along with morula and blastocysts as well (Figure 15E and 15F). All embryos at each stage and each group had similar normal phenotypes except those in the Anti-RBBP4 injected group at the blastocyst stage Figure 16. Our Anti-RBBP4

injected embryos also had a slower development overall compared to the negative control (not shown). When there was a depletion of RBBP4 only 1% of blastocysts developed properly from the morula stage. This 1% most likely represented embryos which had an unbalanced ratio of the 3 components needed for Trim-Away (TRIM21, antibody, and target protein). With each repeat of Trim-Away using anti-RBBP4 injections, there were successful depletions of RBBP4 starting from the 2-cell stage through the blastocyst stage. These results suggest that RBBP4 can be trimmed away as early as the 2-cell stage. It also suggests that with sufficient injected TRIM21- mRNA and antibody, RBBP4 will be depleted causing drastic phenotypic changes within the blastocyst stage.

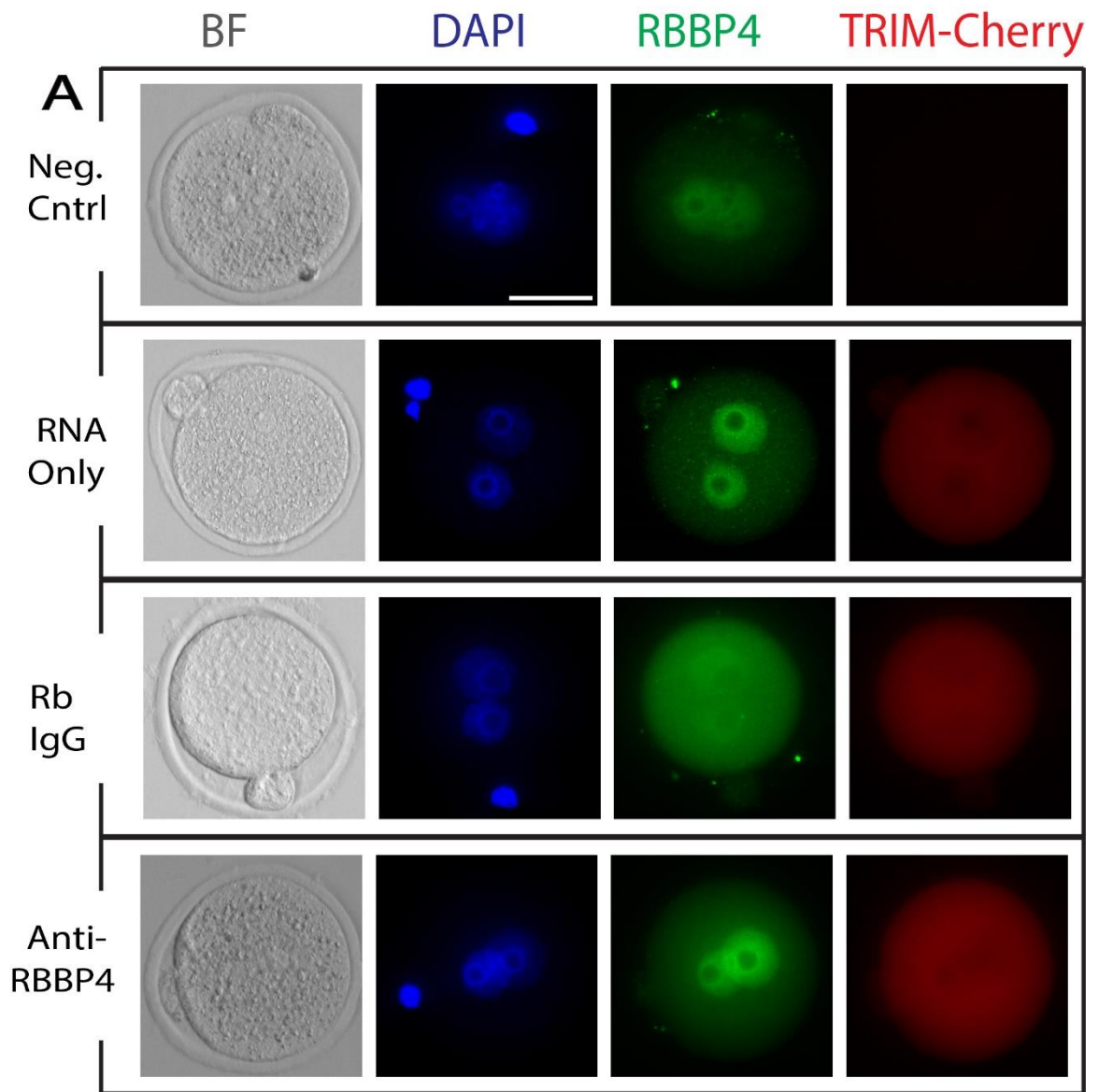


Fig 15A

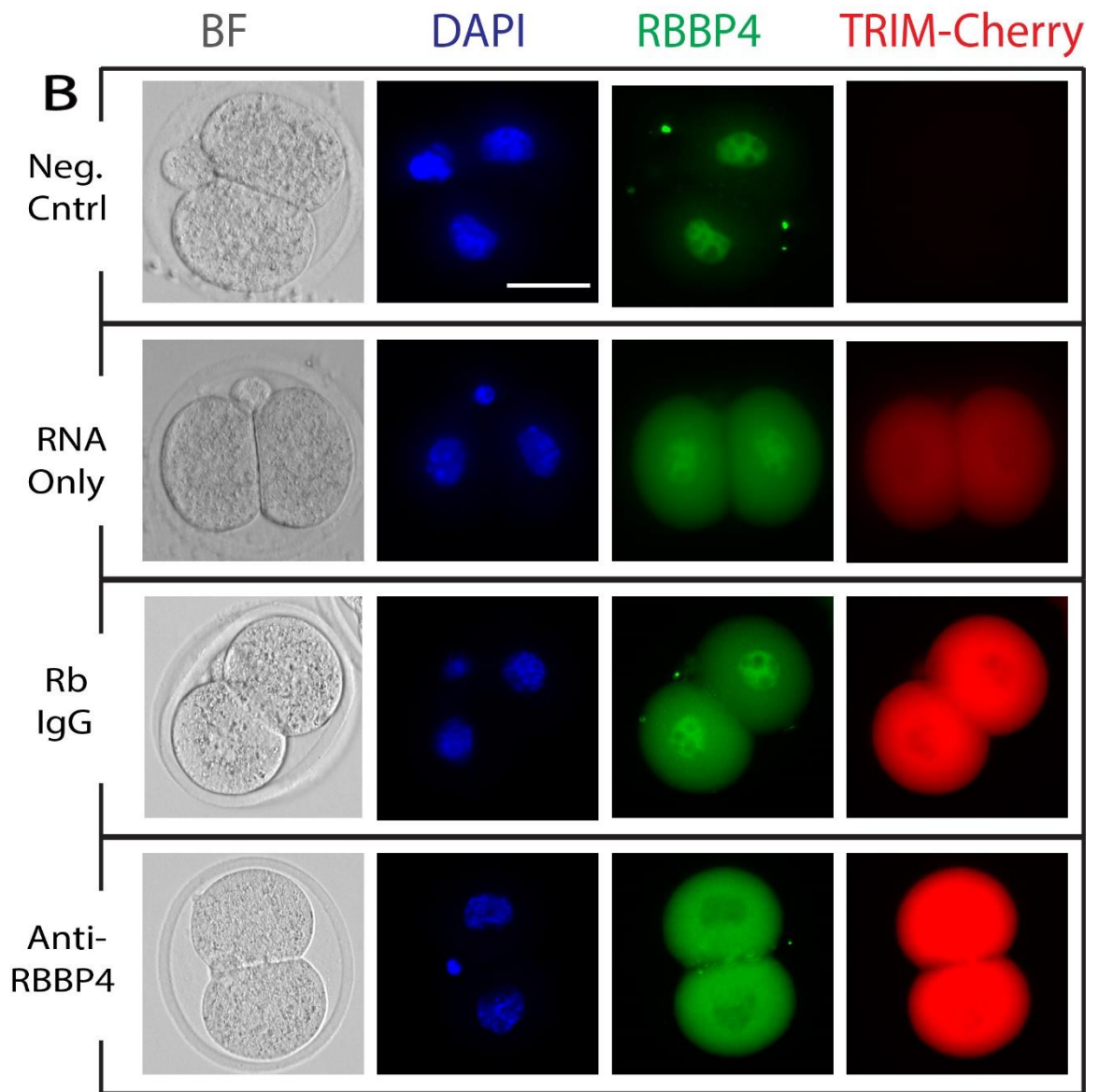


Fig 15B

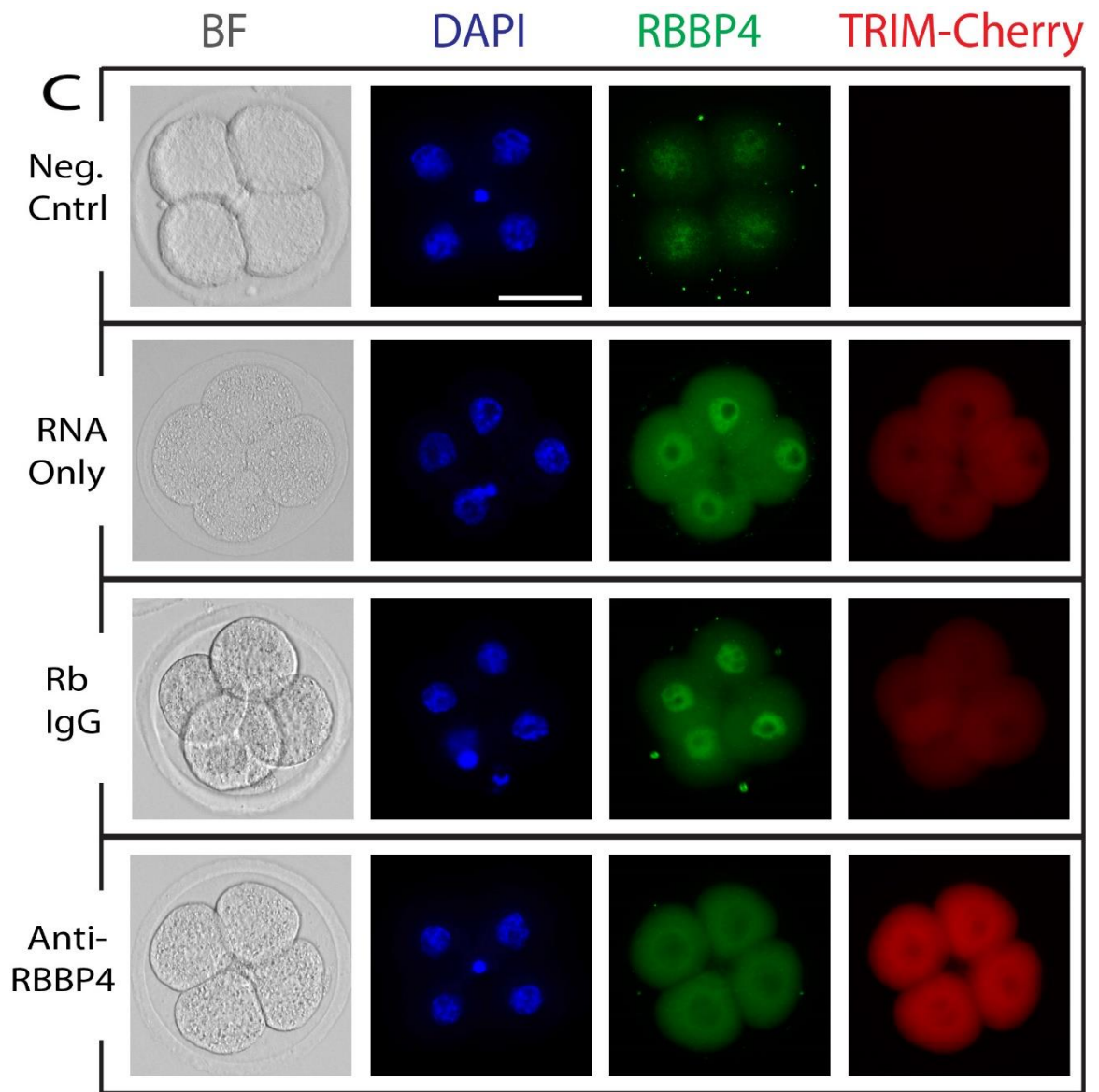


Fig 15C

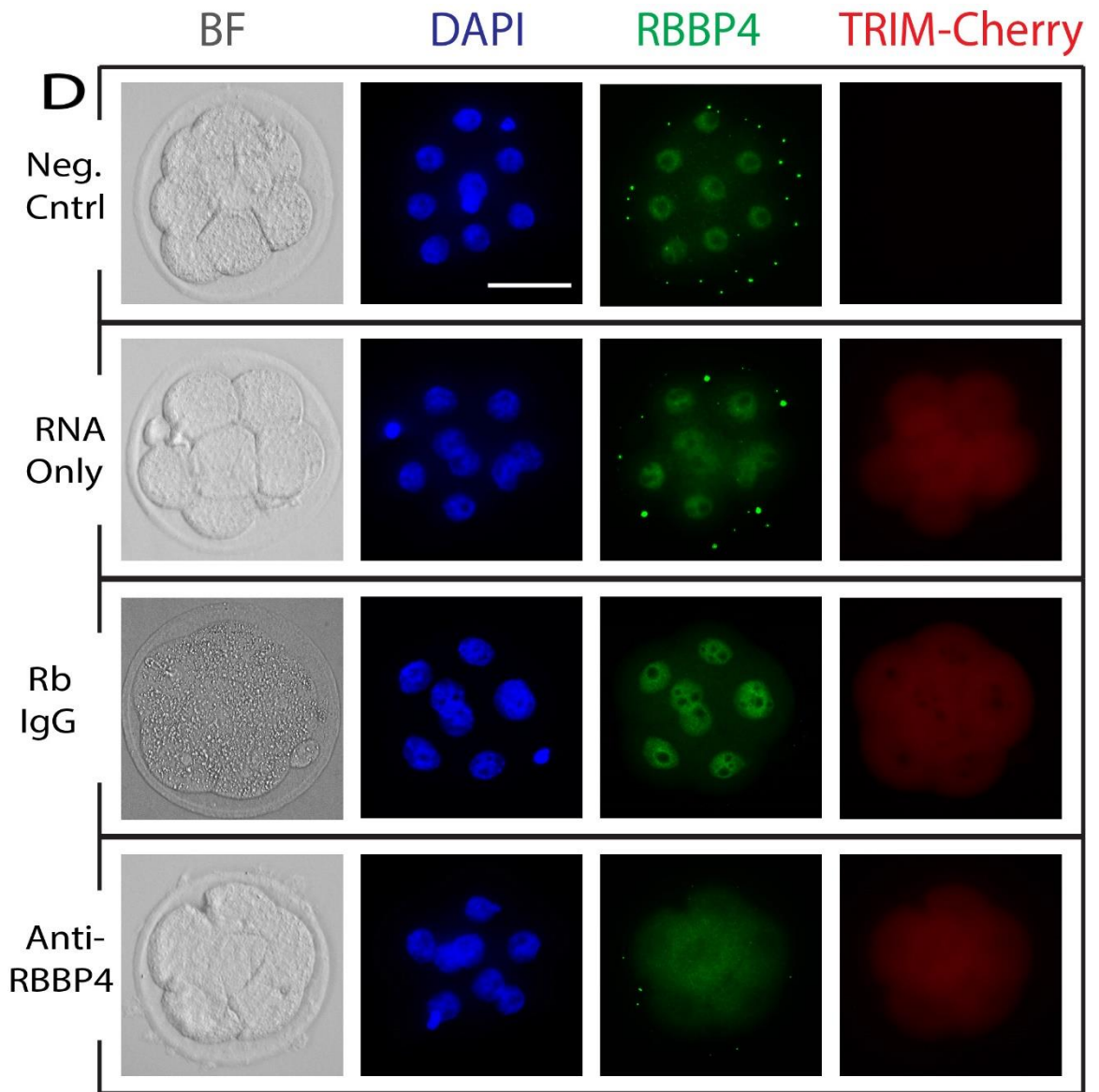


Fig 15D

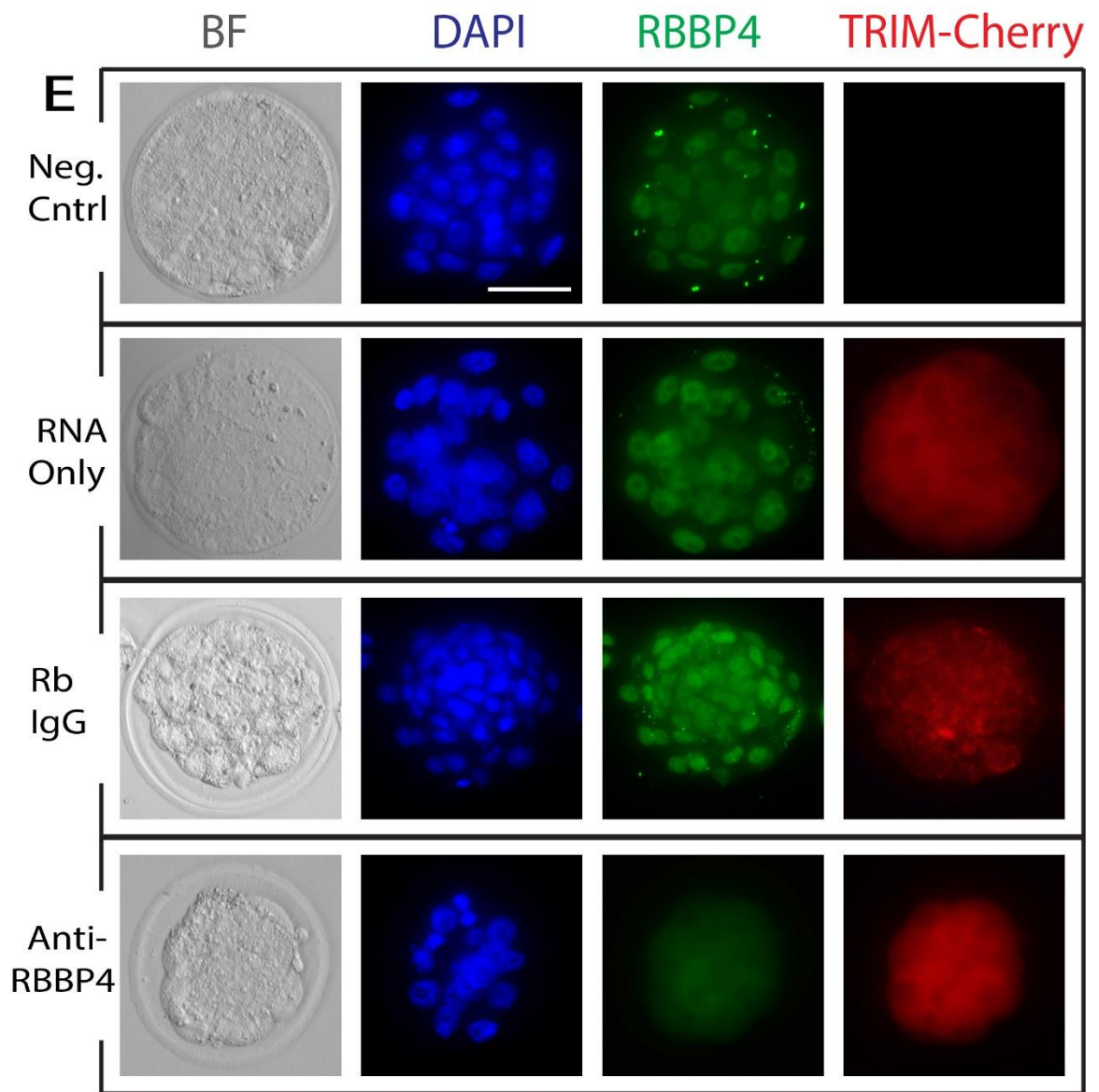


Fig 15E

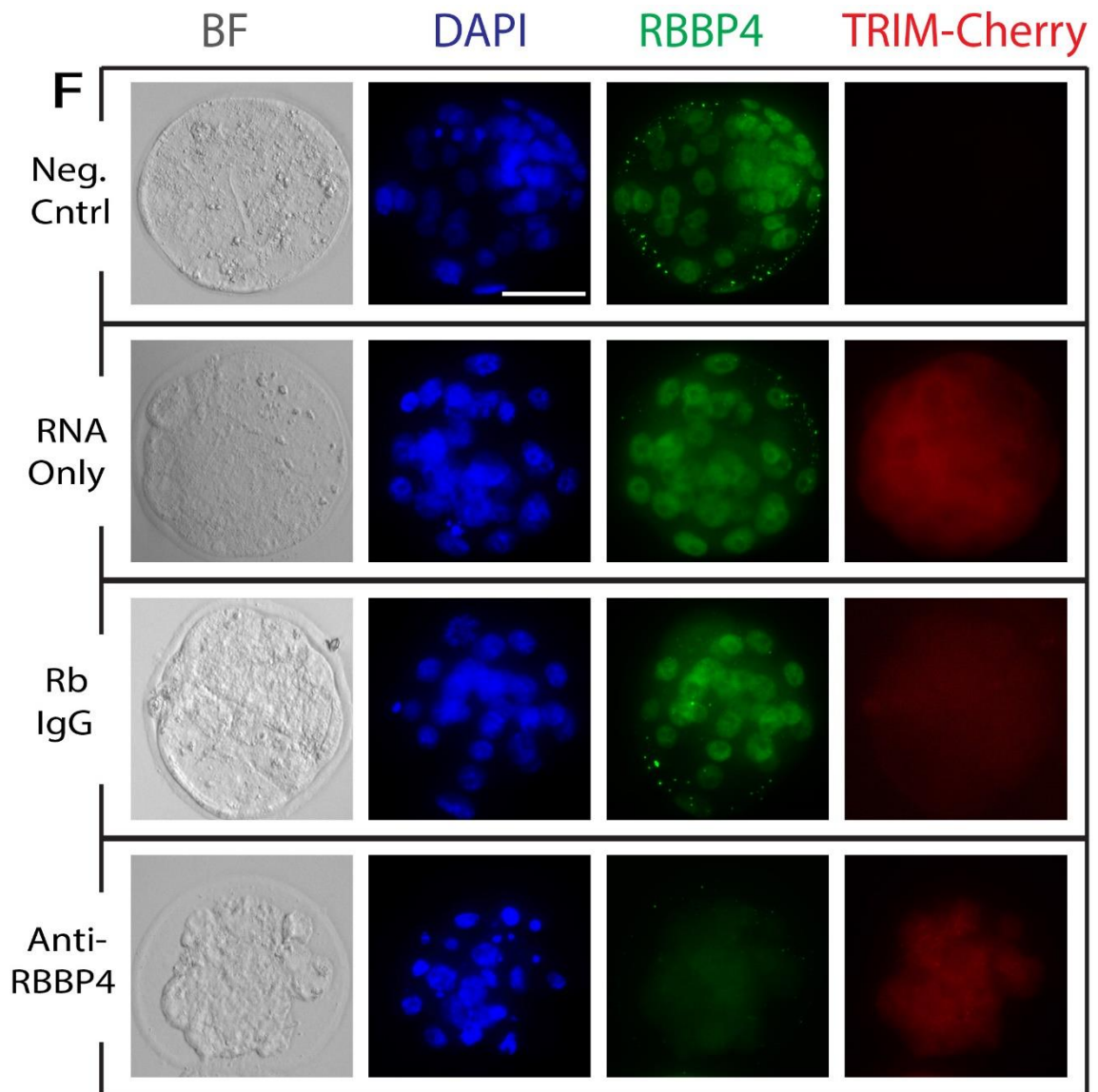


Fig 15A-F. Trim-Away of RBBP4 At All Preimplantation Embryo Development Stages

Anti-RBBP4 was injected 3 hours after injection of mRNA from TRIM21-mCherry . Zygotes were cultured until each developmental stage above was reached and fixed. Immunofluorescence was conducted to observe the concentration of TRIM21 mRNA and RBBP4 protein within each cell. At the zygote stage, there is a clear nuclear signal for RBBP4. In all succeeding embryo development stages, there is no nuclear signal for RBBP4.

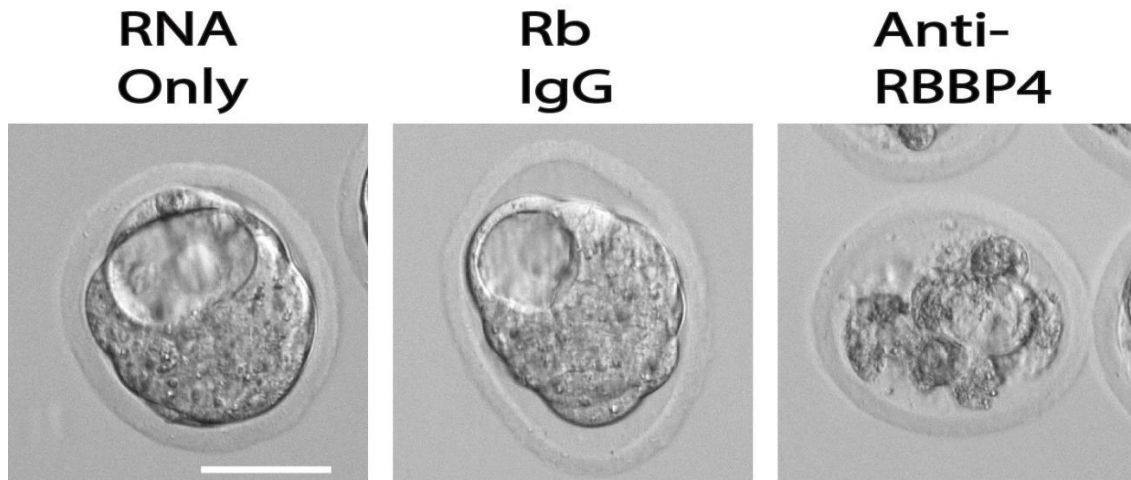


Fig 16. Blastocyst Phenotype

RNA Only and Rb IgG groups formed a blastocoel at the early blastocyst stage. All Anti-RBBP4 injected group were unable to form a blastocoel and had abnormal phenotypes at the early blastocyst stage.

D. Total Nascent RNA

The depletion of RBBP4 through Trim-Away is clear within the embryo starting at the 2-cell stage, and therefore may be affecting different mechanisms within the cell such as transcription and ZGA. To investigate this, we utilized an EU incorporation assay to detect nascent RNA (Figure 17). DNA contains nucleobases such as thymine, guanine, cytosine, and adenine while RNA contains uridine instead of thymine. Within this EU assay, the modified 5-ethynyl uridine (EU) will be incorporated into nascent RNA replacing the natural uridine [46]. The modified nascent RNA will then be detected by the chemoselective ligation reaction between the azide and alkyne. This reaction is detected with the corresponding azide-containing dye (green, fluorescent color). There was little difference in nuclear RNA signal at the 4-cell and 8-cell stage (not shown) from anti-RBBP4 injected embryos compared to our controls of un-injected, RNA Only, and Rb IgG injected embryos. At the 2-cell and Morula stages, un-injected (not shown), RNA Only (not shown), and Rb IgG injected embryos showed high RNA transcription signal

within the nucleus, while anti-RBBP4 injected embryos show much less nuclear signal. These results suggest that RBBP4 has a function in ZGA at the 2-cell stage or gene transcription in later embryo development ZGA.

The EU assay allows for the use of additional probes, such as antibodies. We stained for H4ac and residues (K5, K8, K12, and K16) (Abcam, ab177790). There was no clear difference between control groups and the Anti-RBBP4. Even within each group there were varied signals for H4ac, meaning there will have to be additional studies done to conclude whether RBBP4 has a role in histone acetylation during early embryo development.

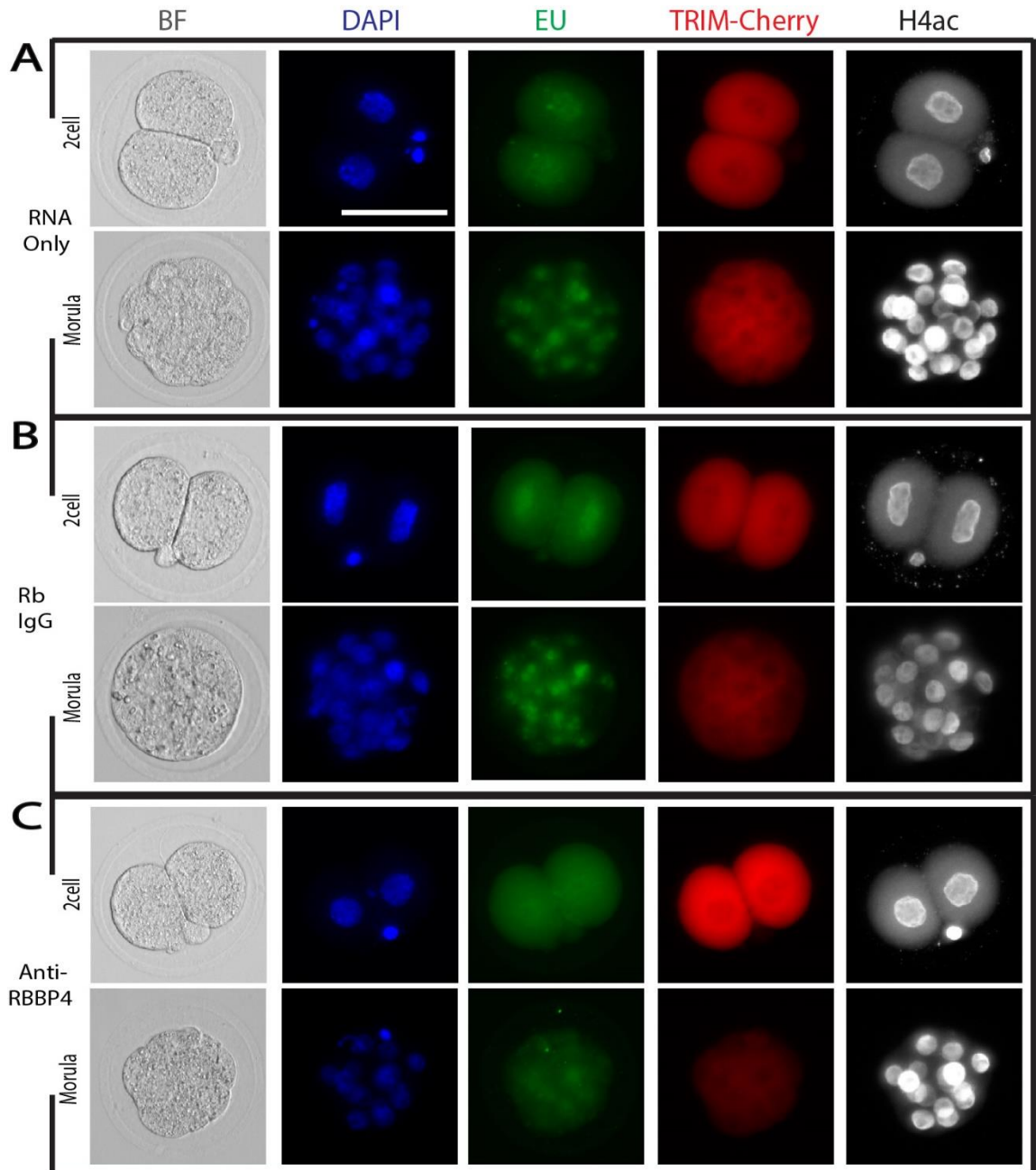


Fig 17. EU Incorporation Assay Analysis

Anti-RBBP4 was injected 3 hours after injection of mRNA from TRIM21-mCherry . Zygotes were incubated at 37°C for until each developmental stage above was reached and were then incubated in KSOM incorporated with EU for 2h. Embryos were immediately fixed and incubated with reaction buffers listed previously. In addition to the EU incorporation, immunofluorescence was conducted to observe the concentration of TRIM21 mRNA and H4ac within each cell.

E. Total Cell Death

The loss of RBBP4 in early embryo development affects successful blastocyst formation and therefore may be caused by high cell death at the Morula stage. To investigate this, we utilized an In Situ Cell Death Detection Kit (Figure 18). This kit is a precise, fast, and simple nonradioactive technique to detect and quantify apoptotic cell death from a molecular level (DNA breaks). DNA breaks were detected with the corresponding label solution (green, fluorescent color). Although this kit is sensitive and aims to reduce background labeling, there was still some background, which is represented by the cytoplasm. At the morula stage, RNA Only embryos and Rb IgG embryos were similar in the amount of cell death present. RNA Only embryos have non-specific binding within their nuclei and cytoplasm along with apoptotic polar bodies and one sperm that was able to penetrate the ZP, but not the zygote itself. Rb IgG embryos also have non-specific binding within the cytoplasm and most of the nuclei, with the exception of only a few nuclei showing the apoptotic signal. Anti-RBBP4 injected embryos had significantly more apoptotic cells especially within most, if not all, nuclei. These results suggest that RBBP4 has a function in DNA repair.

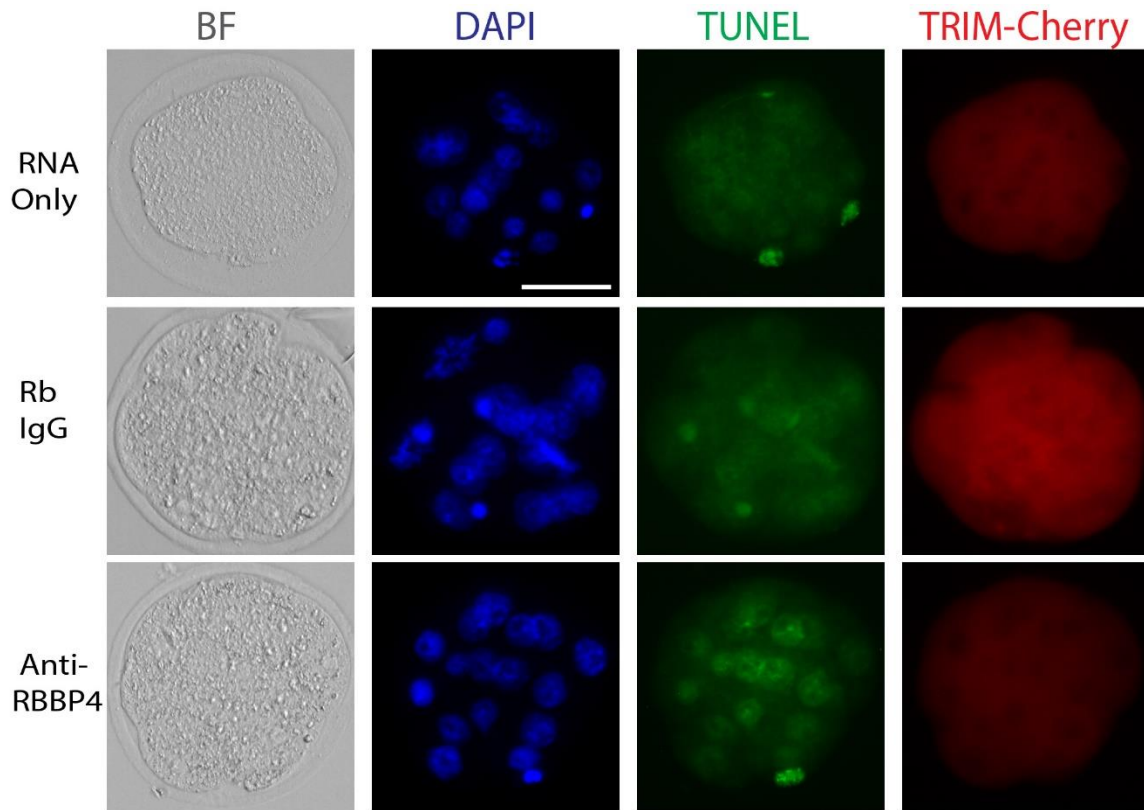


Fig 18. TUNEL of Morula Stage Embryos

Anti-RBBP4 was injected 3 hours after injection of mRNA from TRIM21-mCherry . Zygotes were incubated at 37°C for until the morula stage. Embryos were immediately fixed and incubated with the enzyme solution and label solution.

F. Trim-Away in Oocytes

Previously, a group from Rutgers University studied the loss of RBBP4 in oocyte maturation utilizing an siRNA knockdown (KD). To achieve their KD, they arrested GV oocytes for 12-15 hours. We hypothesized that maybe Trim-Away would be able to deplete RBBP4 earlier than 12-15 when arrested at the GV oocytes stage. Testing this hypothesis, we arrested GV oocytes overnight and saw a small depletion from our group that was fixed after 3h of culture (Figure 19). This slight depletion was most likely due to natural long-term degradation which happens when the freshly made protein is not

shuttled into the nucleus from the cytoplasm because it is being trimmed away immediately by the overexpressed TRIM21 in the cytoplasm. Additionally, our Rb IgG group increased in RBBP4 signal overnight, which was likely due to the cell cycle arrest where new RBBP4 was not being trimmed away and was constantly shuttled into the nucleus.

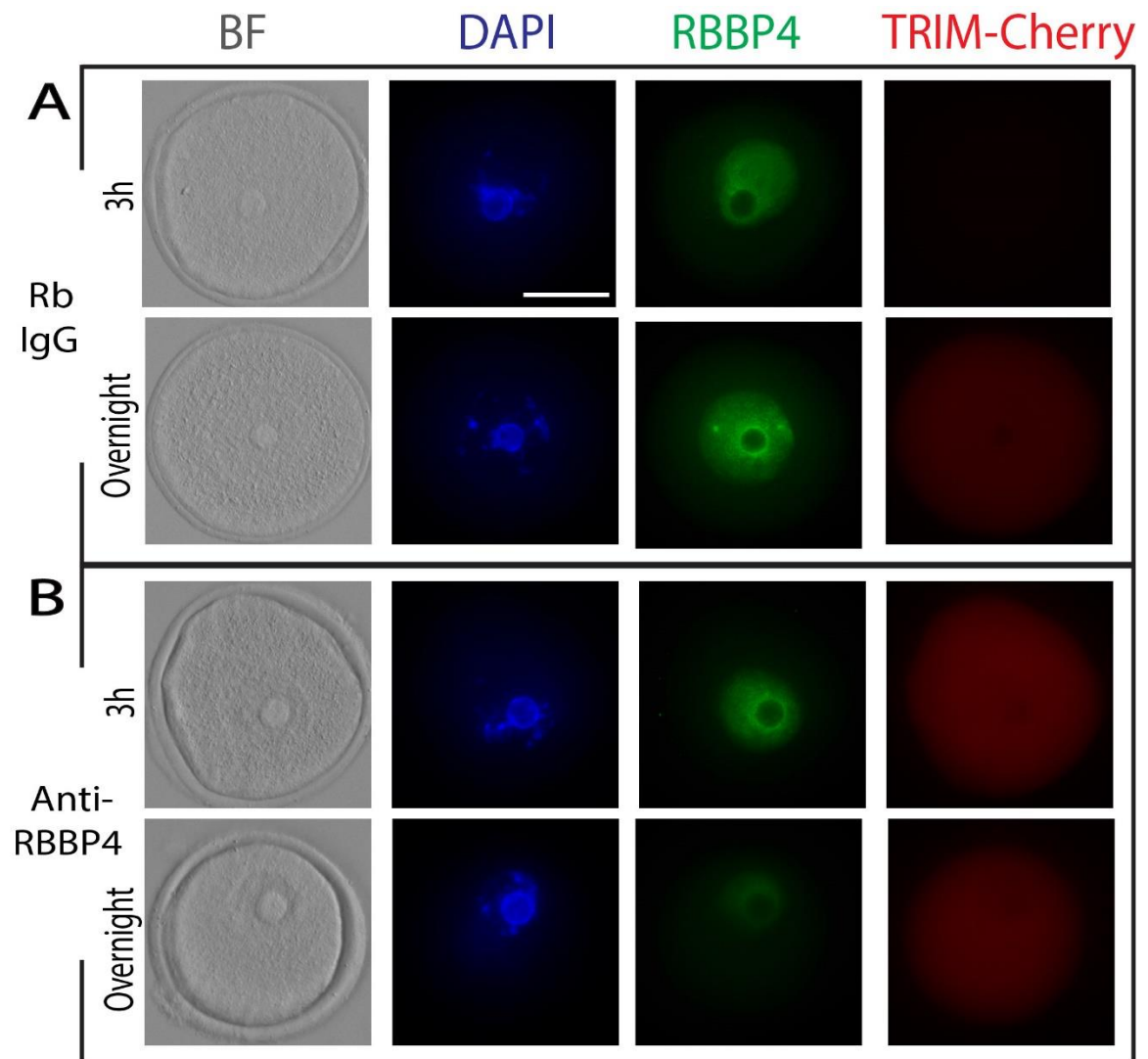


Fig 19. Trim-Away of RBBP4 Using Anti-RBBP4 in Arrested GV Oocytes

Anti-RBBP4 was injected 3 hours after injection of mRNA from pGEMHE-mEGFP-mTRIM21. GV oocytes were cultured for either 3 hours or overnight and then fixed. Immunofluorescence was conducted to observe the concentration of TRIM21 mRNA and RBBP4 protein present. Anti-RBBP4 was purified.

We then wanted to investigate the possibility of depleting RBBP4 at different stages once the oocytes matured in vitro. First, a western blot needed to be run to determine if RBBP4 was present at the MII stage since it is not detectable by IF alone. Un-injected MII oocytes were ran using a Wes machine in the Alfandari lab. The Alfandari lab's main model organism is *Xenopus*, so a test was conducted to quantify how many mouse oocytes would be necessary to see the RBBP4 protein. Serial dilutions were conducted so that in Figure 20, Lane 5 contained 78 oocytes (1X), Lane 6 contained 39 oocytes (1/2X), and Lane 7 contained 19.5 oocytes (1/4X). The least amount of mouse oocytes which can be used for running the Wes machine without a long exposure time is around 39 oocytes, representative in Lane 6. Mouse liver was also used as a positive control for RBBP4. GAPDH, a positive control for all samples and housekeeping gene, was detected in all samples with the proper number of cells (all lanes shown). These results suggest that RBBP4 is present within the MII stage oocyte and that RBBP4 is highly abundant in female germ cells compared to somatic cells of the liver.

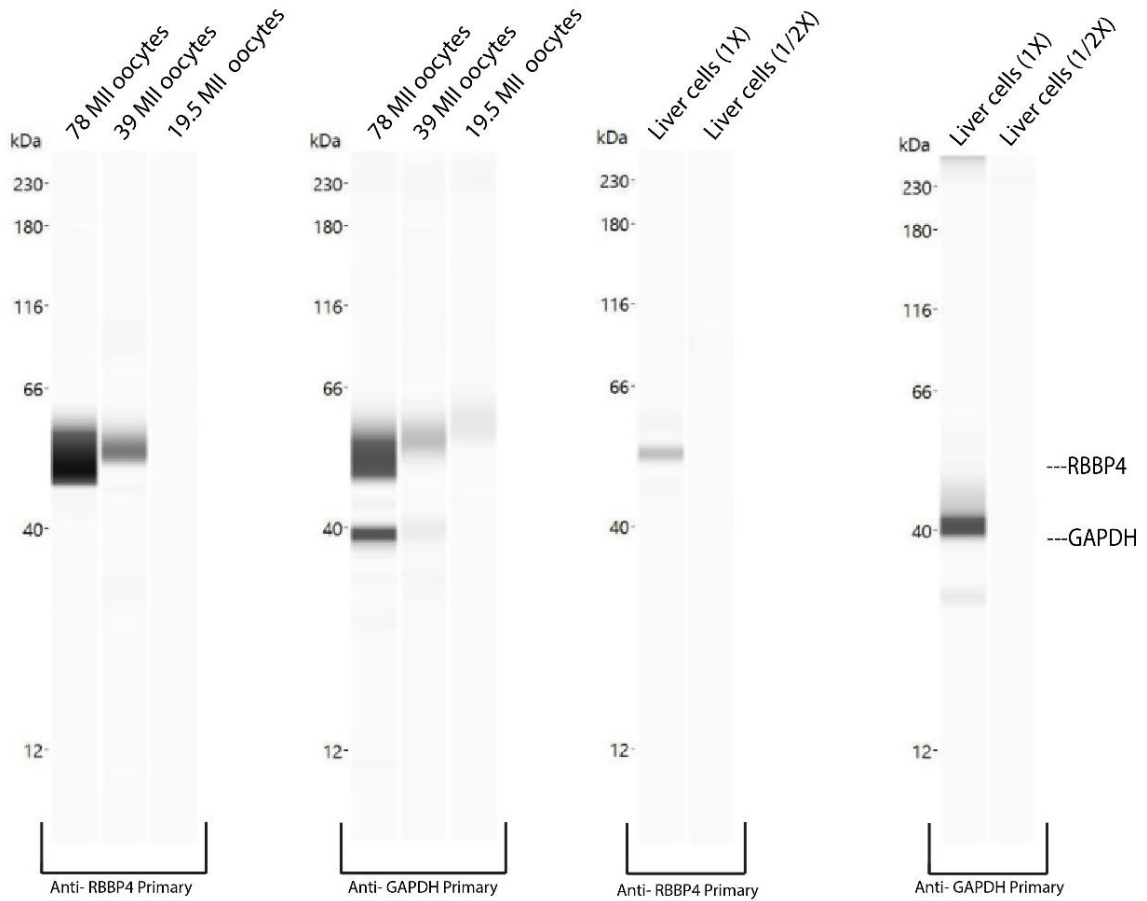


Fig 20. Western Blot for RBBP4 Confirmation

Lane 2-4 represent MII oocytes in serial dilutions from 78 oocytes to 39 oocytes, to 19.5 oocytes detecting for RBBP4 protein. Lane 5-7 represent MII oocytes in serial dilutions from 78 oocytes to 39 oocytes, to 19.5 oocytes detecting for GAPDH protein. Lane 8-9 represents liver cells serial dilutions from the full sample to 1/10th of the sample, detecting for RBBP4 protein. Lane 8-9 represents liver cell serial dilutions from the full sample to 1/10th of the sample, detecting for GAPDH protein. GAPDH represents the positive control for each sample showing there are cells present for each sample provided.

After confirming the necessary number of oocytes to properly run the Wes at a short exposure time, we then collected GV oocytes and co-injected injected TRIM21-mCherry and either anti-RBBP4, Rb IgG, or nothing for a negative control. Co-injection was previously tested within our embryo model because there was a clear depletion with separate injections (not shown). Once we confirmed co-injection trimmed away RBBP4, we conducted these injections into GV oocytes for either 3.5h to the GVBD stage or overnight to the MII stage and then transferred into lysis buffer for a western blot to be ran (Figure 21). Within this western blot, we used a secondary antibody that recognizes the light chain of our injected antibodies, due the possibility of the previous secondary antibody recognizing the injected antibody around the same molecular weight as our RBBP4 protein. The injected antibody will be detected at 25 kDa instead of 50 kDa.

Our GAPDH tested samples showed unclear bands of where GAPDH was located on the molecular weight scale. This was most likely due to the antibody being old or unspecific binding from a long exposure time of the blot. Based on which band is confirmed as GAPDH, our Trim-Away results could change. We also see that there is a shift in protein molecular weight in the MII stage, most likely due to RBBP4 being phosphorylated or compacted in some way.

Although we cannot come to a clear conclusion whether RBBP4 was depleted in our GVBD or MII oocytes, we can see that at the MII stage there is about 3-fold more endogenous RBBP4 protein present than in GVBD oocytes. This was quantified using an electropherogram where GVBD had around a 400 chemiluminescent substrate concentration while MII oocytes had around a 1200 concentration. Using an electropherogram we can quantify lanes 2,3,4, and 5 form the previous western blot

(Figure 22). RBBP4 protein was present within all samples that contained oocytes (seen at 55 kDa). The black peak shown at 55 kDa represents the sample with no oocytes present and confirms the specificity of the Wes machine for detecting RBP4 protein. The light chain of the detected injected antibodies can be seen at 25 kDa and is present in all samples with antibody, except our Anti-RBBP4 injected group. There is a small peak represented showing that there was anti-RBBP4 was present, which suggests that either there was a low concentration of antibody injected and it was not sufficient to deplete RBBP4 or that RBBP4 was too abundant to be depleted at these stages.

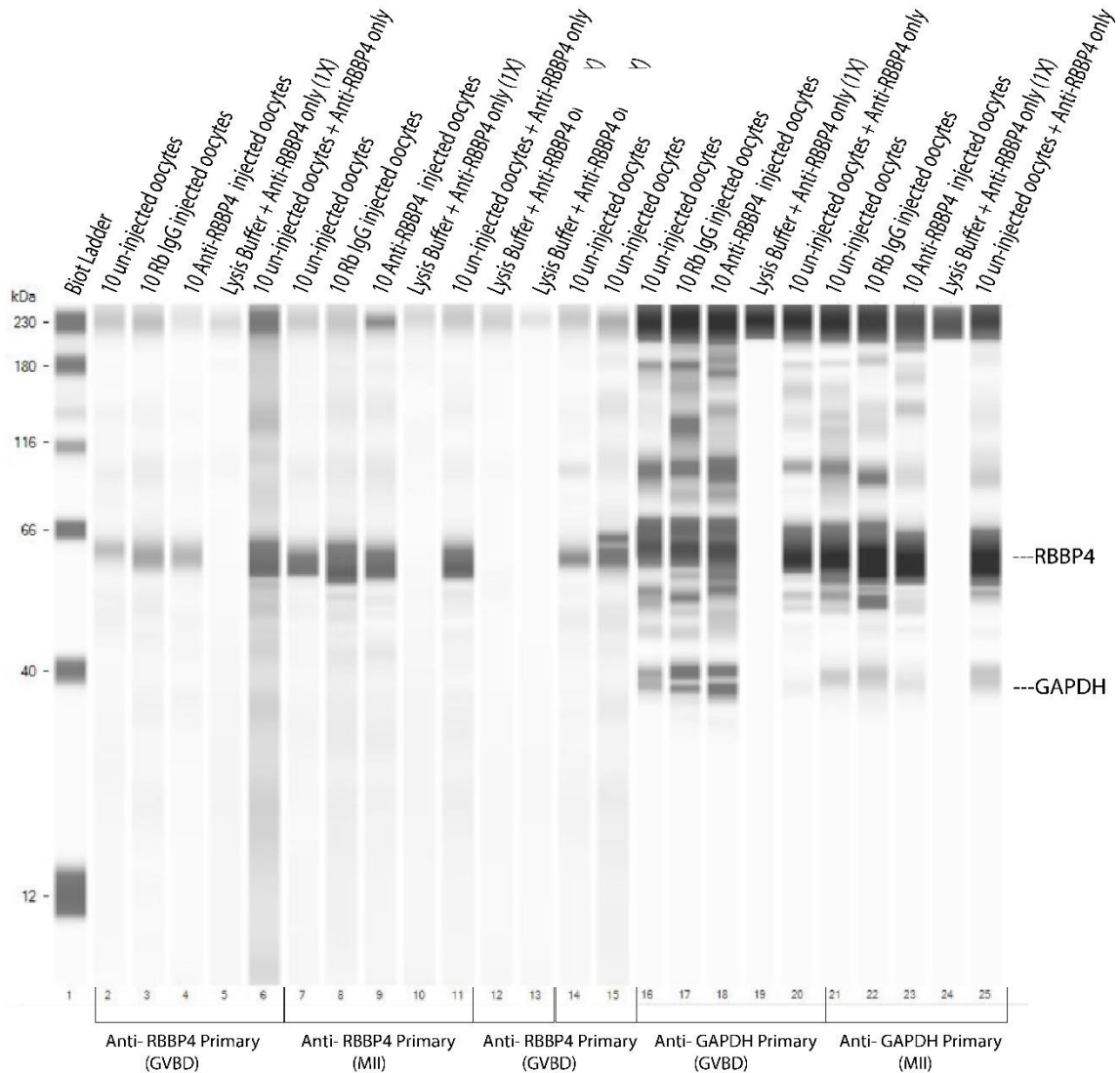


Fig 21. Western Blot for Trim-Away During Oocyte Maturation

All samples containing oocytes used 10 oocytes. Lane 1 represents the biotinylated ladder. Lanes 2-15 represent RBBP4 stained samples. Lanes 16-25 represent GAPDH stained lanes. GAPDH represents the positive control for each sample showing there are cells present for each sample provided. Within lanes 2-6 and 12-20, oocytes were matured from the GV stage to the GVBD stage. Within lanes 7-11 and 21-25 oocytes were matured from the GV stage to the MII stage.

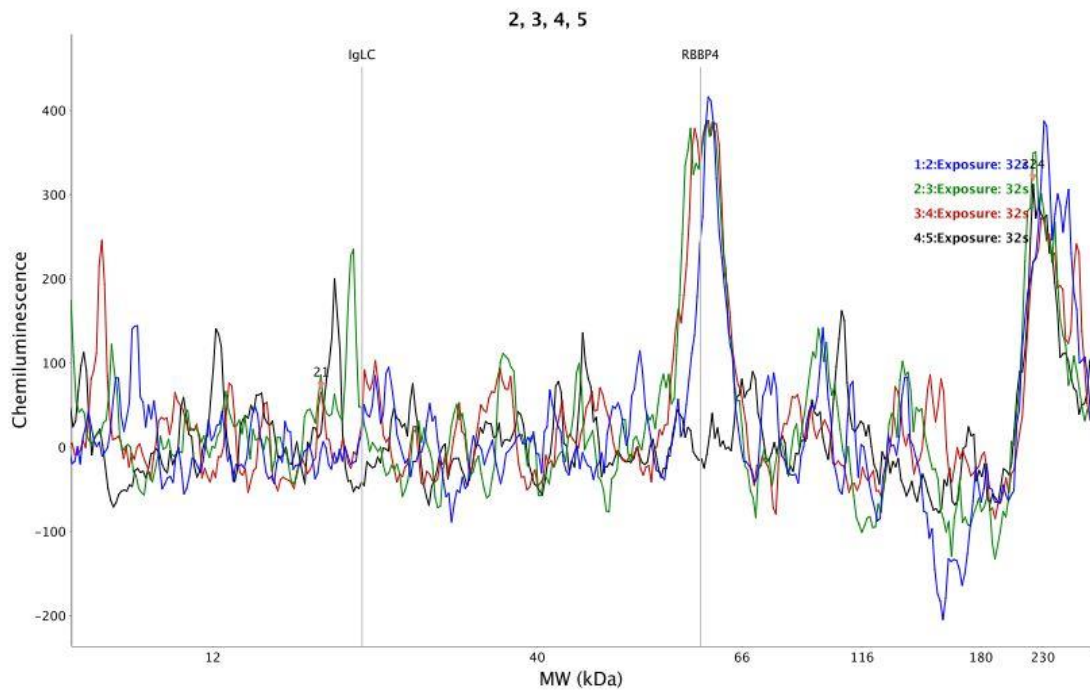


Fig. 22 Electropherogram Quantification

The blue peaks represent un-injected oocytes, green represents Rb IgG injected oocytes, red represents anti-RBBP4 injected oocytes, and black represents our lysis buffer mixed with antibody only. All samples have RBBP4 protein present except the lysis buffer with antibody only (55 kDa). All samples with injected antibody show the antibody present at a high peak except anti-RBBP4 injected oocytes where there is a lower peak (25 kDa).

CHAPTER 4

DISCUSSION

As previously shown in different studies, RBBP4 is essential for oocyte maturation and embryo development. Specifically in oocyte maturation, RBBP4 is essential for histone deacetylation, while in embryo development it is essential for proper segregation of the ICM and TE, and for proper implantation [22, 23]. In many loss of function studies, techniques such as CRISPR/Cas9 and RNAi are used. Unfortunately, these techniques have limitations such as determining an indirect depletion of proteins and the possibility of triggering compensatory mechanisms. A new, acute, and rapid protein depletion method called Trim-Away offers a method to overcome these limitations [34].

Trim-Away utilizes the TRIM21-antibody interaction to target a protein for degradation. Once all 3 components are bound together, the complex is ubiquitinated and dragged to the proteasome for degradation. Trim-Away allows for the depletion of endogenous proteins without the need for prior modification of the protein-coding gene or mRNA [35]. For nuclear proteins, Trim-Away has been seen to accomplish degradation soon after at least one cell division and the TRIM21 mRNA can last for as long as 3-4 days [15]. This technique is flexible and should be able to be applied to any mammalian species. It is also widely applicable due to its ability to be used with many off-the-shelf reagents [35].

One of the most challenging aspects of this project for our lab was the RNA purification process. One critical consideration we did not account for at first was RNases, hydrolytic enzymes that degrade RNA and how easily they can accomplish

this[47, 48]. RNases can be found within solutions, consumables, and labware, and can impact any experiment involving RNA such as *in vitro* transcription (IVT), RNA purification, Ribonuclease Protection Assays (RPAs), and Northern Blots [49]. There are many steps one can take to avoid RNA degradation.

Plasmid purification via Phenol: Chloroform can be useful during the RNA purification processes. Phenol: Chloroform purification of nucleic acids denatures proteins and collects the organic phase (interphase) for use in RNA purification. The Phenol: Chloroform protocol used from Thermo Fisher has been tested and no RNase or DNase activity was detected [49]. This protocol provided us with successful and consistent results of plasmid purification. Our RNA purification results with plasmid purification compared to unpurified plasmids were drastically different and more consistent in providing high concentrations of purified RNA, so the decision to always purify plasmids via Phenol: Chloroform before IVT was made.

Additionally, RNase activity can be limited by RNaseZap, an RNase Decontamination Solution (ThermoFisher, AM9782). This solution is sprayed onto glass and plastic surfaces to decontaminate and destroy RNases on contact. RNaseZap has been proven to be more effective at removing high levels of RNase contamination than other products and can be applied to microcentrifuge tubes without inhibiting subsequent enzymatic reactions, which is why we choose this product to eliminate RNases [48].

RNA purification also relies on high graded ethanol for adding into the samples and for precipitation. The MEGAclean Transcription Clean-Up Kit we used, requires 100% ethanol (ACS grade or better). With the combination of our plasmid purification,

spraying RNaseZap onto our workspaces, and new ACS grade ethanol, we were able to successfully repeat multiple RNA purifications for mRNA injections.

Even though our microinjection machinery is high end, there is no way to inject the exact same amount of mRNA each time, we can only aim for this which contributed to the different TRIM21 overexpression signals we see throughout all figures in this thesis. As far as degradation of each component goes, all 3 components in the Trim-Away mechanism, TRIM21, antibody, and the endogenous target protein, will be degraded by the proteasome [50]. Additionally, our mRNA that was first being injected for separate injections (mRNA then antibody 3h later) was at a concentration of 750 ng/ μ L. We realized this high concentration was not feasible for proper embryo development, and subsequently lowered our mRNA concentration by diluting our samples with nuclease-free water. We found that around 300 ng/ μ L for separate mRNA and antibody injections allowed proper embryo development. Our co-injection experiments consisted of injecting half mRNA and half desired antibody simultaneously, which meant we needed to increase the mRNA concentration to 600 ng/ μ L.

Co-injections for GV oocytes did not provide sufficient depletion of RBBP4 in the beginning of this project. At first, our co-injection experiments showed no TRIM21 protein translated from the injected mRNA. We hypothesized this was either due to our mRNA quality or due our commercial antibody for RBBP4 [51]. After conducting a run of GV oocyte separate injections, we confirmed it was not our mRNA quality, but due to our antibody. Purification of anti-RBBP4 was completed and injected into GV oocytes 3h after mRNA with similar results of no RBBP4 depletion. Based on the original Trim-Away paper by Clift and colleagues, at least one cell division cycle must occur to allow

the degradation of retained nuclear target proteins [50]. When at least one cell cycle division was considered for embryo development, RBBP4 was depleted as early as the 2-cell stage. Within future experiments it may be useful to utilize nanobodies for the depletion of nuclear proteins if no cell division will occur for arrested GV oocytes. The Fc domain of our commercial antibody would be fused to the nanobody for TRIM21 to bind to, and the nanobody would be able to infiltrate the nucleus without nuclear membrane breakdown [35].

Previously, the Cui Lab collaborated with Dr. Jesse Mager's Lab (University of Massachusetts Amherst) to study RBBP4 using a KO model and determined RBBP4 was important for embryo development [23]. Since RBBP4 is a lethal gene, a heterozygous-by-heterozygous breeding scheme was needed and there was always maternally loaded RBBP4 mRNA and protein. It was not until 3 days after blastocyst collection, during the outgrowth phase, did we see an abnormal phenotype in the KO embryos. Here we report that there was a depletion of RBBP4 by the 2-cell stage that causes an abnormal phenotype at the early blastocyst stage. Studying the depletion of RBBP4 via Trim-Away has an advantage over the CRISPR/Cas9 KO model used since it can cause an earlier, more severe phenotype and overcome the above mentioned maternal loading limitation.

Using an EU Incorporation Assay and a TUNNEL Assay, we investigated the reason behind our abnormal blastocyst development. Sha and colleagues used a similar EU Assay to measure the amount of nascent RNA by using Trim-Away for protein depletion of BTG4. This group did not see any changes in RNA synthesis within the Trim-Away of BTG4 at the 2-cell stage [52]. Our Trim-Away model for depletion of RBBP4 showed a significant decrease in nascent RNA at the 2-cell and morula embryo

stages, compared to the clear signal in the control groups of RNA only and Rb IgG injection. This suggests that RBBP4 has a function in either ZGA or gene transcription in later stages of embryo development. Through a TUNEL Assay, Miao and colleagues saw an increased apoptotic signal within their homozygous KO embryos at the blastocyst stage [23]. Similarly, in our TUNEL Assay, we saw a significant increase in apoptotic cell within the morula stage within our anti-RBBP4 injected group and the control RNA Only and Rb IgG groups, suggesting that RBBP4 has a role in DNA repair during early embryogenesis.

Within many experiments, the cytoplasm brightness of Rb IgG injected embryos overlaid, or dulled, the RBBP4 nuclear signal. We hypothesized this was due to the Rb IgG binding our secondary antibody (anti-rabbit) within the IF process. We saw similar cytoplasmic brightness within the RNA Only group and hypothesized this was due to TRIM21 binding to the secondary antibody during IF as well. Through a trial run of injecting less Rb IgG and less TRIM21 mRNA, we discovered that both the injected antibody and TRIM21 can bind to the secondary antibody during IF, causing this high cytoplasmic signal. Additionally, any “leftover” injected anti-RBBP4 that was not degraded by the proteasome when Trim-Away machinery depleted the RBBP4 protein, also could bind to the secondary antibody of IF.

Although an endogenous RBBP4 signal is visible at all stages of embryo development, this is not the case for mouse oocyte maturation. During oocyte maturation RBBP4 signal is visible via IF at the GV stage, while at the MI and MII stages it is not [22]. This is most likely due to RBBP4 modification within the oocyte at these stages. RBBP4 being localized to the chromatin and being found in many other protein

complexes such as the HDAC, NuRD, and PCR2 could have an impact on this [24-26]. There is a possibility RBBP4 may be phosphorylated or compacted in a way such that our commercial antibody cannot detect the protein's immunogen. Commercial antibodies bind to a specific immunogen from a POI. Our anti-RBBP4 specifically binds to human RBBP4 amino acids 1-100 (N terminal) and is reactive with mouse, rat, and human [51]. It is possible RBBP4 may be undetectable within rat and human MI and MII oocytes as well. Similarly, in our H2B experiments, H2B was not detected through IF at the MII stage and was not depleted long term through Trim-Away either. This was most likely due to the same reason of this protein being modified, for example phosphorylated, or compacted in a way it was not able to bind to our commercial antibody for H2B but could bind to our GFP antibody. The MAP4 protein did not seem to have this issue when trimming away during the MII oocyte stage and could be trimmed away with either anti-MAP4 or anti-GFP.

To overcome the limitation of RBBP4 not being detectable by IF, a western blot was run via the Wes machine in the Alfandari lab (University of Massachusetts Amherst) and confirmed RBBP4 was present within the MII oocyte stage and was more abundant in female germ cells compared to liver somatic cells. Through western blot experiments we discovered that RBBP4 was not fully depleted in oocytes and that there is a possibility RBBP4 is too abundant at these stages for the concentration of antibody we injected. There was also a shift in molecular weight most likely due to this modification on RBBP4. With the RBBP4 concentration shown in each band, we concluded RBBP4 was about 3-fold higher in MII oocytes than GVBD oocytes. Within future experiments we hope to find the reason our protein was not fully depleted in oocytes and then hopefully

both embryo and oocyte Trim-Away models can be applied to many other species or eventually aid in human health.

In conclusion our results showed that RBBP4 is required for proper blastocyst development and RBBP4 is more abundant in MII oocytes than GVBD oocytes. We also report that the loss of RBBP4 hinders RNA synthesis and causes cell death in later stages of embryo development. Lastly, while our Trim-Away methodology can deplete RBBP4 as early as the 2-cell stage in embryos, our oocyte Trim-Away protocol needs to be optimized.

BIBLIOGRAPHY

1. Homer, H.A., et al., *Restaging the spindle assembly checkpoint in female mammalian meiosis I*. Cell Cycle, 2005. **4**(5): p. 650-3.
2. Calarco, P.G., *Centrosome precursors in the acentriolar mouse oocyte*. Microsc Res Tech, 2000. **49**(5): p. 428-34.
3. Tosti, E., *Calcium ion currents mediating oocyte maturation events*. Reprod Biol Endocrinol, 2006. **4**: p. 26.
4. Pomerantz, Y. and N. Dekel, *Molecular participants in regulation of the meiotic cell cycle in mammalian oocytes*. Reprod Fertil Dev, 2013. **25**(3): p. 484-94.
5. Virant-Klun, I., et al., *Identification of Maturation-Specific Proteins by Single-Cell Proteomics of Human Oocytes*. Mol Cell Proteomics, 2016. **15**(8): p. 2616-27.
6. Namgoong, S. and N.H. Kim, *Meiotic spindle formation in mammalian oocytes: implications for human infertility*. Biol Reprod, 2018. **98**(2): p. 153-161.
7. Tartia, A.P., et al., *Cell volume regulation is initiated in mouse oocytes after ovulation*. Development, 2009. **136**(13): p. 2247-54.
8. Mihajlovic, A.I. and G. FitzHarris, *Segregating Chromosomes in the Mammalian Oocyte*. Curr Biol, 2018. **28**(16): p. R895-R907.
9. Madgwick, S. and K.T. Jones, *How eggs arrest at metaphase II: MPF stabilisation plus APC/C inhibition equals Cytostatic Factor*. Cell Div, 2007. **2**: p. 4.
10. Verlhac, M.H. and M.E. Terret, *Oocyte Maturation and Development*. F1000Res, 2016. **5**.
11. Greaney, J., Z. Wei, and H. Homer, *Regulation of chromosome segregation in oocytes and the cellular basis for female meiotic errors*. Hum Reprod Update, 2018. **24**(2): p. 135-161.
12. Zhou, C.J., et al., *Loss of CENPF leads to developmental failure in mouse embryos*. Cell Cycle, 2019. **18**(20): p. 2784-2799.
13. Carroll, J., et al., *Spatiotemporal dynamics of intracellular [Ca²⁺]_i oscillations during the growth and meiotic maturation of mouse oocytes*. Development, 1994. **120**(12): p. 3507-17.
14. Monteiro-Riviere, N.A., et al., *Interspecies and interregional analysis of the comparative histologic thickness and laser Doppler blood flow measurements at five cutaneous sites in nine species*. J Invest Dermatol, 1990. **95**(5): p. 582-6.

15. Roth, S., L.J. Fulcher, and G.P. Sapkota, *Advances in targeted degradation of endogenous proteins*. Cell Mol Life Sci, 2019. **76**(14): p. 2761-2777.
16. Chazaud, C. and Y. Yamanaka, *Lineage specification in the mouse preimplantation embryo*. Development, 2016. **143**(7): p. 1063-74.
17. Shen-Orr, S.S., Y. Pilpel, and C.P. Hunter, *Composition and regulation of maternal and zygotic transcriptomes reflects species-specific reproductive mode*. Genome Biol, 2010. **11**(6): p. R58.
18. Condic, M.L., *The Role of Maternal-Effect Genes in Mammalian Development: Are Mammalian Embryos Really an Exception?* Stem Cell Rev Rep, 2016. **12**(3): p. 276-84.
19. Ancelin, K., et al., *Maternal LSD1/KDM1A is an essential regulator of chromatin and transcription landscapes during zygotic genome activation*. Elife, 2016. **5**.
20. Menchero, S., et al., *Signaling pathways in mammalian preimplantation development: Linking cellular phenotypes to lineage decisions*. Dev Dyn, 2017. **246**(4): p. 245-261.
21. Schultz, R.M., *Regulation of zygotic gene activation in the mouse*. Bioessays, 1993. **15**(8): p. 531-8.
22. Balboula, A.Z., et al., *RBBP4 regulates histone deacetylation and bipolar spindle assembly during oocyte maturation in the mouse*. Biol Reprod, 2015. **92**(4): p. 105.
23. Miao, X., et al., *Loss of RBBP4 results in defective inner cell mass, severe apoptosis, hyperacetylated histones and preimplantation lethality in micedagger*. Biol Reprod, 2020. **103**(1): p. 13-23.
24. Kaji, K., et al., *The NuRD component Mbd3 is required for pluripotency of embryonic stem cells*. Nat Cell Biol, 2006. **8**(3): p. 285-92.
25. Mager, J., et al., *Genome imprinting regulated by the mouse Polycomb group protein Eed*. Nat Genet, 2003. **33**(4): p. 502-7.
26. Taunton, J., C.A. Hassig, and S.L. Schreiber, *A mammalian histone deacetylase related to the yeast transcriptional regulator Rpd3p*. Science, 1996. **272**(5260): p. 408-11.
27. Kitange, G.J., et al., *Retinoblastoma Binding Protein 4 Modulates Temozolomide Sensitivity in Glioblastoma by Regulating DNA Repair Proteins*. Cell Rep, 2016. **14**(11): p. 2587-98.
28. Pavlopoulos, E., et al., *Molecular mechanism for age-related memory loss: the histone-binding protein RbAp48*. Sci Transl Med, 2013. **5**(200): p. 200ra115.

29. Schultz, L.E., et al., *Epigenetic regulators Rbbp4 and Hdac1 are overexpressed in a zebrafish model of RB1 embryonal brain tumor, and are required for neural progenitor survival and proliferation*. *Dis Model Mech*, 2018. **11**(6).
30. Tsujii, A., et al., *Retinoblastoma-binding Protein 4-regulated Classical Nuclear Transport Is Involved in Cellular Senescence*. *J Biol Chem*, 2015. **290**(49): p. 29375-88.
31. Liu, C., et al., *Predator: A novel method for targeted protein degradation*. *bioRxiv*, 2020: p. 2020.07.31.231787.
32. Foss, S., et al., *TRIM21-From Intracellular Immunity to Therapy*. *Front Immunol*, 2019. **10**: p. 2049.
33. Luh, L.M., et al., *Prey for the Proteasome: Targeted Protein Degradation-A Medicinal Chemist's Perspective*. *Angew Chem Int Ed Engl*, 2020. **59**(36): p. 15448-15466.
34. Prozzillo, Y., et al., *Targeted Protein Degradation Tools: Overview and Future Perspectives*. *Biology (Basel)*, 2020. **9**(12).
35. Clift, D., et al., *A Method for the Acute and Rapid Degradation of Endogenous Proteins*. *Cell*, 2017. **171**(7): p. 1692-1706 e18.
36. Camlin, N.J. and J.P. Evans, *Auxin-inducible protein degradation as a novel approach for protein depletion and reverse genetic discoveries in mammalian oocytesdagger*. *Biol Reprod*, 2019. **101**(4): p. 704-718.
37. Dean, D.A., *Brenner's Encyclopedia of Genetics (Second Edition): Microinjection*, K.H. Stanley Maloy, Editor. 2013, Academic Press. p. 409-410.
38. Kaustubh A. Jinturkar, M.N.R., Ambikanandan Misra, *Challenges in Delivery of Therapeutic Genomics and Proteomics: Gene Delivery Using Physical Methods*, A. Misra, Editor. 2011. p. 83-126.
39. Zeng, J. and L.C. James, *Intracellular antibody immunity and its applications*. *PLoS Pathog*, 2020. **16**(8): p. e1008657.
40. TherapeuticAntibodyEngineering, *Antibody Interactions with the Immune System*, L.M.S. William R. Strohl, Editor. 2012, Woodhead Publishing p. 131-595.
41. McEwan, W.A. and L.C. James, *TRIM21-dependent intracellular antibody neutralization of virus infection*. *Prog Mol Biol Transl Sci*, 2015. **129**: p. 167-87.
42. Mallery, D.L., et al., *Antibodies mediate intracellular immunity through tripartite motif-containing 21 (TRIM21)*. *Proc Natl Acad Sci U S A*, 2010. **107**(46): p. 19985-90.

43. Du, S., et al., *Cell-Permeant Bioadaptors for Cytosolic Delivery of Native Antibodies: A "Mix-and-Go" Approach*. ACS Cent Sci, 2020. **6**(12): p. 2362-2376.
44. Addgene. *TRIM21 Plasmids*. 2021 [cited 2021 March 23].
45. NewEnglandBiolabs. *NEBuffer Activity/Performance Chart with Restriction Enzymes*. 2021; Available from: <https://www.neb.com/tools-and-resources/usage-guidelines/nebuffer-performance-chart-with-restriction-enzymes>.
46. JenaBioscience. *5-Ethynyl-uridine (5-EU)*. 2021 [cited 2021 April 25]; Available from: <https://www.jenabioscience.com/click-chemistry/click-reagents-by-application/on-rna/global-rna-synthesis-monitoring/clk-n002-5-ethynyl-uridine-5-eu>.
47. AgScientific. *Introduction to RNase*. 2021 [cited 2021 April 20]; Available from: <https://agscientific.com/blog/2019/05/rnase-a-faq/>.
48. BioRad. *What is Real-Time PCR 9qPCR)?* 2021 [cited 2021 April 20]; Available from: <https://www.bio-rad.com/en-us/applications-technologies/what-real-time-pcr-qpcr?ID=LUSO4W8UU#3>.
49. ThermoFisher. *RNaseZap™ RNase Decontamination Solution*. 2021 [cited 2021 April 30]; Available from: <https://www.thermofisher.com/order/catalog/product/AM9782#/AM9782>.
50. Clift, D., et al., *Acute and rapid degradation of endogenous proteins by Trim-Away*. Nat Protoc, 2018. **13**(10): p. 2149-2175.
51. Abcam. *Recombinant Anti-RBBP4 antibody [EPR3411] - ChIP Grade (ab79416)*. 2021 [cited 2021 March 15]; Available from: <https://www.abcam.com/rbbp4-antibody-epr3411-chip-grade-ab79416.html?productWallTab=ShowAll>.
52. Sha, Q.Q., et al., *Characterization of zygotic genome activation-dependent maternal mRNA clearance in mouse*. Nucleic Acids Res, 2020. **48**(2): p. 879-894.